

## Accelerated Article Preview

# Striking antibody evasion manifested by the Omicron variant of SARS-CoV-2

---

Received: 14 December 2021

---

Accepted: 23 December 2021

---

Accelerated Article Preview

---

Published online: 23 December 2021

---

Cite this article as: Liu, L. et al. Striking antibody evasion manifested by the Omicron variant of SARS-CoV-2. *Nature* <https://doi.org/10.1038/d41586-021-03826-3> (2021).

---

Lihong Liu, Sho Iketani, Yicheng Guo, Jasper F-W. Chan, Maple Wang, Liyuan Liu, Yang Luo, Hin Chu, Yiming Huang, Manoj S. Nair, Jian Yu, Kenn K-H. Chik, Terrence T-T. Yuen, Chaemin Yoon, Kelvin K-W. To, Honglin Chen, Michael T. Yin, Magdalena E. Sobieszczyk, Yaoxing Huang, Harris H. Wang, Zizhang Sheng, Kwok-Yung Yuen & David D. Ho

---

This is a PDF file of a manuscript that has been peer reviewed and accepted for publication in *Nature* and is provided in this format here as a response to the exceptional public-health crisis. This accepted manuscript will continue through the processes of copy editing and formatting to publication of a finalized version of record on nature.com. Please note there may be errors present in this version, which may affect the content, and all legal disclaimers apply.

ACCELERATED ARTICLE PREVIEW

## Striking Antibody Evasion Manifested by the Omicron Variant of SARS-CoV-2

1 Lihong Liu<sup>1\*</sup>, Sho Iketani<sup>1,2\*</sup>, Yicheng Guo<sup>1\*</sup>, Jasper F-W. Chan<sup>3,4\*</sup>, Maple Wang<sup>1\*</sup>, Liyuan  
2 Liu<sup>5\*</sup>, Yang Luo<sup>1</sup>, Hin Chu<sup>3,4</sup>, Yiming Huang<sup>5</sup>, Manoj S. Nair<sup>1</sup>, Jian Yu<sup>1</sup>, Kenn K-H. Chik<sup>4</sup>,  
3 Terrence T-T. Yuen<sup>3</sup>, Chaemin Yoon<sup>3</sup>, Kelvin K-W. To<sup>3,4</sup>, Honglin Chen<sup>3,4</sup>, Michael T. Yin<sup>1,6</sup>,  
4 Magdalena E. Sobieszczyk<sup>1,6</sup>, Yaoxing Huang<sup>1</sup>, Harris H. Wang<sup>5</sup>, Zizhang Sheng<sup>1</sup>,  
5 Kwok-Yung Yuen<sup>3,4</sup>, David D. Ho<sup>1,2,6^</sup>  
6

7 <sup>1</sup>Aaron Diamond AIDS Research Center, Columbia University Vagelos College of Physicians and  
8 Surgeons, New York, NY 10032, USA

9 <sup>2</sup>Department of Microbiology and Immunology, Columbia University Vagelos College of  
10 Physicians and Surgeons, New York, NY 10032, USA

11 <sup>3</sup>State Key Laboratory of Emerging Infectious Diseases, Carol Yu Centre for Infection,  
12 Department of Microbiology, Li Ka Shing Faculty of Medicine, The University of Hong Kong,  
13 Pokfulam, Hong Kong Special Administrative Region, China

14 <sup>4</sup>Centre for Virology, Vaccinology and Therapeutics, Hong Kong Science and Technology Park,  
15 Hong Kong Special Administrative Region, China

16 <sup>5</sup>Department of Systems Biology, Columbia University Vagelos College of Physicians and  
17 Surgeons, New York, NY 10032, USA

18 <sup>6</sup>Division of Infectious Diseases, Department of Medicine, Columbia University Vagelos College  
19 of Physicians and Surgeons, New York, NY 10032, USA  
20

21 \* These authors contributed equally

22 ^ Address correspondence to David D. Ho ([dh2994@cumc.columbia.edu](mailto:dh2994@cumc.columbia.edu), 212-304-6101, 701 W  
23 168th St, 11th Floor, New York, NY 10032)  
24

25 Word count: 3617

26 **Abstract**

27

28 The Omicron (B.1.1.529) variant of SARS-CoV-2 (severe acute respiratory syndrome coronavirus  
29 2) was only recently detected in southern Africa, but its subsequent spread has been extensive,  
30 both regionally and globally<sup>1</sup>. It is expected to become dominant in the coming weeks<sup>2</sup>, probably  
31 due to enhanced transmissibility. A striking feature of this variant is the large number of spike  
32 mutations<sup>3</sup> that pose a threat to the efficacy of current COVID-19 (coronavirus disease 2019)  
33 vaccines and antibody therapies<sup>4</sup>. This concern is amplified by the findings from our study. We  
34 found B.1.1.529 to be markedly resistant to neutralization by serum not only from convalescent  
35 patients, but also from individuals vaccinated with one of the four widely used COVID-19 vaccines.  
36 Even serum from persons vaccinated and boosted with mRNA-based vaccines exhibited  
37 substantially diminished neutralizing activity against B.1.1.529. By evaluating a panel of  
38 monoclonal antibodies to all known epitope clusters on the spike protein, we noted that the activity  
39 of 17 of the 19 antibodies tested were either abolished or impaired, including ones currently  
40 authorized or approved for use in patients. In addition, we also identified four new spike mutations  
41 (S371L, N440K, G446S, and Q493R) that confer greater antibody resistance to B.1.1.529. The  
42 Omicron variant presents a serious threat to many existing COVID-19 vaccines and therapies,  
43 compelling the development of new interventions that anticipate the evolutionary trajectory of  
44 SARS-CoV-2.

45

## 46 **Main text**

47 The COVID-19 (coronavirus disease 2019) pandemic rages on, as the causative agent, SARS-  
48 CoV-2 (severe acute respiratory syndrome coronavirus 2), continues to evolve. Many diverse viral  
49 variants have emerged (**Fig. 1a**), each characterized by mutations in the spike protein that raise  
50 concerns of both antibody evasion and enhanced transmission. The Beta (B.1.351) variant was  
51 found to be most refractory to antibody neutralization<sup>4</sup> and thus compromised the efficacy of  
52 vaccines<sup>5-7</sup> and therapeutic antibodies. The Alpha (B.1.1.7) variant became dominant globally in  
53 early 2021 due to an edge in transmission<sup>8</sup> only to be replaced by the Delta (B.1.617.2) variant,  
54 which exhibited even greater propensity to spread coupled with a moderate level of antibody  
55 resistance<sup>9</sup>. Then came the Omicron (B.1.1.529) variant, first detected in southern Africa in  
56 November 2021<sup>3,10,11</sup> (**Fig. 1a**). It has since spread rapidly in the region, as well as to over 60  
57 countries, gaining traction even where the Delta variant is prevalent. The short doubling time (2-  
58 3 days) of Omicron cases suggests it could become dominant soon<sup>2</sup>. Moreover, its spike protein  
59 contains an alarming number of >30 mutations (**Fig. 1b and Extended Data Fig. 1**), including at  
60 least 15 in the receptor-binding domain (RBD), the principal target for neutralizing antibodies.  
61 These extensive spike mutations raise the specter that current vaccines and therapeutic antibodies  
62 would be greatly compromised. This concern is amplified by the findings we now report.

## 64 **Serum neutralization of B.1.1.529**

65 We first examined the neutralizing activity of serum collected in the Spring of 2020 from COVID-  
66 19 patients, who were presumably infected with the wild-type SARS-CoV-2 (9-120 days post-  
67 symptoms) (see Methods and **Extended Data Table 1**). Samples from 10 individuals were tested  
68 for neutralization against both D614G (WT) and B.1.1.529 pseudoviruses. While robust titers  
69 were observed against D614G, a significant drop (>32-fold) in ID<sub>50</sub> (50% infectious dose) titers  
70 was observed against B.1.1.529, with only 2 samples showing titers above the limit of detection  
71 (LOD) (**Fig. 1c and Extended Data Fig. 2a**). We then assessed the neutralizing activity of sera  
72 from individuals who received one of the four widely used COVID-19 vaccines: BNT162b2  
73 (Pfizer, 15-213 days post-vaccination), mRNA-1273 (Moderna, 6-177 days post-vaccination),  
74 Ad26.COV2.S (Johnson & Johnson, 50-186 days post-vaccination), and ChAdOx1 nCoV-19  
75 (AstraZeneca, 91-159 days post-vaccination) (see Methods and **Extended Data Table 2**). In all  
76 cases, a substantial loss in neutralizing potency was observed against B.1.1.529 (**Fig. 1d and**

77 **Extended Data Fig. 2b-f).** For the two mRNA-based vaccines, BNT162b2 and mRNA-1273, a  
78 >21-fold and >8.6-fold decrease in ID<sub>50</sub> was seen, respectively. We note that, for these two groups,  
79 we specifically chose samples with high titers such that the fold-change in titer could be better  
80 quantified, so the difference in the number of samples having titers above the LOD (6/13 for  
81 BNT162b2 versus 11/12 for mRNA-1273) may be favorably biased. Within the Ad26.COV2.S  
82 and ChAdOx1 nCOV-19 groups, all samples were below the LOD against B.1.1.529, except for  
83 two Ad26.COV2.S samples from patients with a previous history of SARS-CoV-2 infection (**Fig.**  
84 **1d**). Collectively, these results suggest that individuals who were previously infected or fully  
85 vaccinated remain at risk for B.1.1.529 infection.

86

87 Booster shots are now routinely administered in many countries 6 months after full vaccination.  
88 Therefore, we also examined the serum neutralizing activity of individuals who had received three  
89 homologous mRNA vaccinations (13 with BNT162b2 and 2 with mRNA-1273, 14-90 days post-  
90 vaccination). Every sample showed lower activity in neutralizing B.1.1.529, with a mean drop of  
91 6.5-fold compared to WT (**Fig. 1d**). Although all samples had titers above the LOD, the substantial  
92 loss in activity may still pose a risk for B.1.1.529 infection despite the booster vaccination.

93

94 We then confirmed the above findings by testing a subset of the BNT162b2 and mRNA-1273  
95 vaccinee serum samples using authentic SARS-CoV-2 isolates: wild type and B.1.1.529. Again,  
96 a substantial decrease in neutralization of B.1.1.529 was observed, with mean drops of >6.0-fold  
97 and >4.1-fold for the fully vaccinated group and the boosted group, respectively (**Fig. 1e**).

98

### 99 **Antibody neutralization of B.1.1.529**

100 To understand the types of antibodies in serum that lost neutralizing activity against B.1.1.529, we  
101 assessed the neutralization profile of 19 well-characterized monoclonal antibodies (mAbs) to the  
102 spike protein, including 17 directed to RBD and 2 directed to the N-terminal domain (NTD). We  
103 included mAbs that have been authorized or approved for clinical use, either individually or in  
104 combination: REGN10987 (imdevimab)<sup>12</sup>, REGN10933 (casirivimab)<sup>12</sup>, COV2-2196  
105 (tixagevimab)<sup>13</sup>, COV2-2130 (cilgavimab)<sup>13</sup>, LY-CoV555 (bamlanivimab)<sup>14</sup>, CB6 (etesevimab)<sup>15</sup>,  
106 Brii-196 (amubarvimab)<sup>16</sup>, Brii-198 (romlusevimab)<sup>16</sup>, and S309 (sotrovimab)<sup>17</sup>. We also  
107 included other mAbs of interest: 910-30<sup>18</sup>, ADG-2<sup>19</sup>, DH1047<sup>20</sup>, S2X259<sup>21</sup>, and our antibodies 1-

108 20, 2-15, 2-7, 4-18, 5-7, and 10-40<sup>22-24</sup>. The footprints of mAbs with structures available were  
109 drawn in relation to the mutations found in B.1.1.529 RBD (**Fig. 2a**) and NTD (**Fig. 2b**). The risk  
110 to each of the 4 classes<sup>25</sup> of RBD mAbs, as well as to the NTD mAbs, was immediately apparent.  
111 Indeed, neutralization studies on B.1.1.529 pseudovirus showed that 17 of the 19 mAbs tested lost  
112 neutralizing activity completely or partially (**Fig. 2c and Extended Data Fig. 3**). The potency of  
113 class 1 and class 2 RBD mAbs all dropped by >100-fold, as did the more potent mAbs in RBD  
114 class 3 (REGN10987, COV2-2130, and 2-7). The activities of S309 and Brie-198 were spared.  
115 All mAbs in RBD class 4 lost neutralization potency against B.1.1.529 by at least 10-fold, as did  
116 mAb directed to the antigenic supersite<sup>26</sup> (4-18) or the alternate site<sup>23</sup> (5-7) on NTD. Strikingly,  
117 all four combination mAb drugs in clinical use lost substantial activity against B.1.1.529, likely  
118 abolishing or impairing their efficacy in patients.

119  
120 Approximately 10% of the B.1.1.529 viruses in GISAID<sup>1</sup> (Global Initiative on Sharing All  
121 Influenza Data) also contain an additional RBD mutation, R346K, which is the defining mutation  
122 for the Mu (B.1.621) variant<sup>27</sup>. We therefore constructed another pseudovirus (B.1.1.529+R346K)  
123 containing this mutation for additional testing using the same panel of mAbs (**Fig. 2d**). The overall  
124 findings resembled those already shown in **Fig. 2c**, with the exception that the neutralizing activity  
125 of Brie-198 was abolished. In fact, nearly the entire panel of antibodies was essentially rendered  
126 inactive against this minor form of the Omicron variant.

127  
128 The fold changes in IC<sub>50</sub> of the mAbs against B.1.1.529 and B.1.1.529+R346K relative to D614G  
129 are summarized in the first two rows of **Fig. 3a**. The remarkable loss of activity observed for all  
130 classes of mAbs against B.1.1.529 suggest that perhaps the same is occurring in the serum of  
131 convalescent patients and vaccinated individuals.

### 132 133 **Mutations conferring antibody resistance**

134 To understand the specific B.1.1.529 mutations that confer antibody resistance, we next tested  
135 individually the same panel of 19 mAbs against pseudoviruses for each of the 34 mutations  
136 (excluding D614G) found in B.1.1.529 or B.1.1.529+R346K. Our findings not only confirmed the  
137 role of known mutations at spike residues 142-145, 417, 484, and 501 in conferring resistance to  
138 NTD or RBD (class 1 or class 2) antibodies<sup>4</sup> but also revealed several mutations that were

139 previously not known to have functional importance to neutralization (**Fig. 3a and Extended Data**  
140 **Fig. 4**). Q493R, previously shown to affect binding of CB6 and LY-CoV555<sup>28</sup> as well as  
141 polyclonal sera<sup>29</sup>, mediated resistance to CB6 (class 1) as well as to LY-CoV555 and 2-15 (class  
142 2), findings that could be explained by the abolishment of hydrogen bonds due to the long side  
143 chain of arginine and induced steric clashes with CDRH3 in these antibodies (**Fig. 3b, left panels**).  
144 Both N440K and G446S mediated resistance to REGN10987 and 2-7 (class 3), observations that  
145 could also be explained by steric hindrance (**Fig. 3b, middle panels**). The most striking and  
146 perhaps unexpected finding was that S371L broadly affected neutralization by mAbs in all 4 RBD  
147 classes (**Fig. 3a and Extended Data Fig. 4**). While the precise mechanism of this resistance is  
148 unknown, in silico modeling suggested two possibilities (**Fig. 3b, right panels**). First, in the RBD-  
149 down state, mutating Ser to Leu results in an interference with the N343 glycan, thereby possibly  
150 altering its conformation and affecting class 3 antibodies that typically bind this region. Second,  
151 in the RBD-up state, S371L may alter the local conformation of the loop consisting of S371-S373-  
152 S375, thereby affecting the binding of class 4 antibodies that generally target a portion of this  
153 loop<sup>24</sup>. It is not clear how class 1 and class 2 RBD mAbs are affected by this mutation.

154

### 155 **Evolution of SARS-CoV-2 to antibodies**

156 To gain insight into the antibody resistance of B.1.1.529 relative to previous SARS-CoV-2 variants,  
157 we evaluated the neutralizing activity of the same panel of neutralizing mAbs against  
158 pseudoviruses for B.1.1.7<sup>8</sup>, B.1.526<sup>30</sup>, B.1.429<sup>31</sup>, B.1.617.2<sup>9</sup>, P.1<sup>32</sup>, and B.1.351<sup>33</sup>. It is evident  
159 from these results (**Fig. 4 and Extended Data Fig. 5**) that previous variants developed resistance  
160 only to NTD antibodies and class 1 and class 2 RBD antibodies. Here B.1.1.529, with or without  
161 R346K, has made a big mutational leap by becoming not only nearly completely resistant to class  
162 1 and class 2 RBD antibodies, but also substantial resistance to both class 3 and class 4 RBD  
163 antibodies. B.1.1.529 is now the most complete “escapee” from neutralization by currently  
164 available antibodies.

165

### 166 **Discussion**

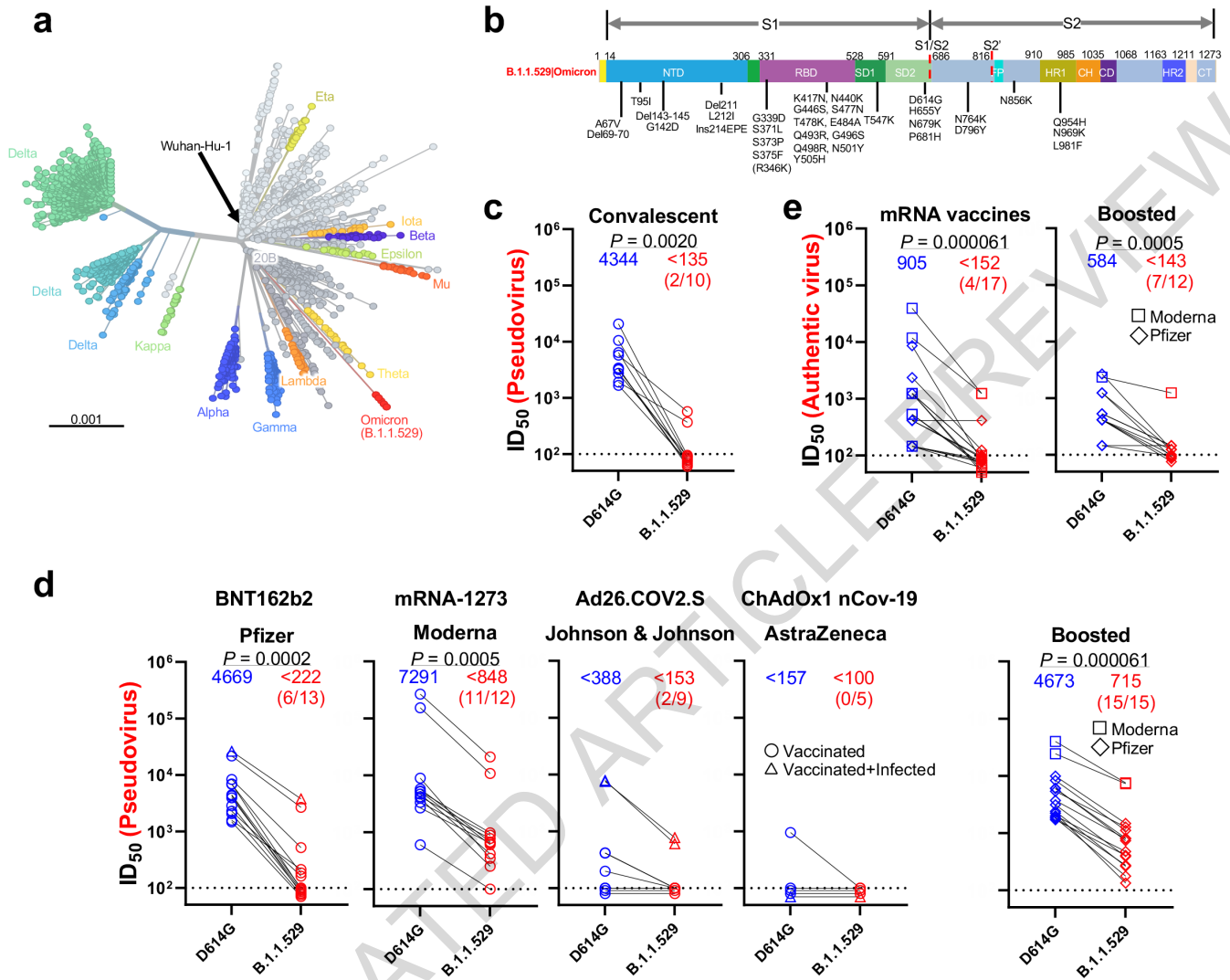
167 The Omicron variant struck fear almost as soon as it was detected to be spreading in South Africa.  
168 That this new variant would transmit more readily has come true in the ensuing weeks<sup>2</sup>. The  
169 extensive mutations found in its spike protein raised concerns that the efficacy of current COVID-

170 19 vaccines and antibody therapies might be compromised. Indeed, in this study, sera from  
171 convalescent patients (**Fig. 1c**) and vaccinees (**Figs. 1d and 1e**) showed markedly reduced  
172 neutralizing activity against B.1.1.529. Other studies have found similar losses<sup>34-38</sup>. These  
173 findings are in line with emerging clinical data on the Omicron variant demonstrating higher rates  
174 of reinfection<sup>11</sup> and vaccine breakthroughs. In fact, recent reports showed that the efficacy of two  
175 doses of BNT162b2 vaccine has dropped from over 90% against the original SARS-CoV-2 strain  
176 to approximately 40% and 33% against B.1.1.529 in the United Kingdom<sup>39</sup> and South Africa<sup>40</sup>,  
177 respectively. Even a third booster shot may not adequately protect against Omicron infection<sup>39,41</sup>,  
178 although the protection against disease still makes it advisable to administer booster vaccinations.  
179 Vaccines that elicited lower neutralizing titers<sup>35,42</sup> are expected to fare worse against B.1.1.529.

180  
181 The nature of the loss in serum neutralizing activity against B.1.1.529 could be discerned from our  
182 findings on a panel of mAbs directed to the viral spike. The neutralizing activities of all four major  
183 classes of RBD mAbs and two distinct classes of NTD mAbs are either abolished or impaired  
184 (**Figs. 2c and 2d**). In addition to previously identified mutations that confer antibody resistance<sup>4</sup>,  
185 we have uncovered four new spike mutations with functional consequences. Q493R confers  
186 resistance to some class 1 and class 2 RBD mAbs; N440K and G446S confer resistance to some  
187 class 3 RBD mAbs; and S371L confers global resistance to many RBD mAbs via mechanisms that  
188 are not yet apparent. While performing these mAb studies, we also observed that nearly all the  
189 currently authorized or approved mAb drugs are rendered weak or inactive by B.1.1.529 (**Figs. 2c**  
190 **and 3a**). In fact, the Omicron variant that contains R346K almost flattens the antibody therapy  
191 landscape for COVID-19 (**Fig. 2d and 3a**).

192  
193 The scientific community has chased after SARS-CoV-2 variants for a year. As more and more  
194 of them appeared, our interventions directed to the spike became increasingly ineffective. The  
195 Omicron variant has now put an exclamation mark on this point. It is not too far-fetched to think  
196 that this SARS-CoV-2 is now only a mutation or two away from being pan-resistant to current  
197 antibodies, either monoclonal or polyclonal. We must devise strategies that anticipate the  
198 evolutionary direction of the virus and develop agents that target better conserved viral elements.

**Fig. 1**

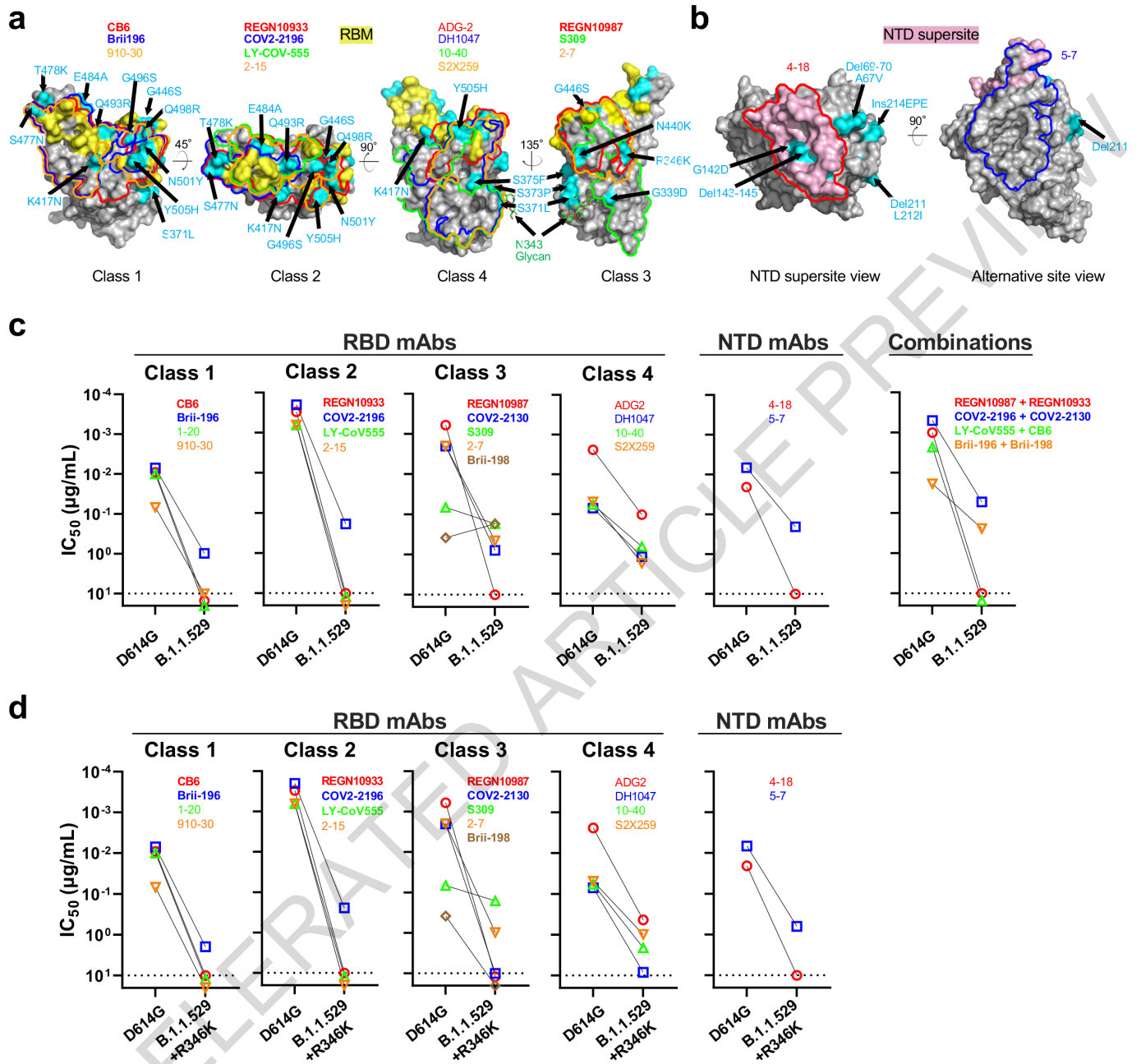


199 **Figure Legends**

200  
201  
202  
203  
204  
205  
206  
207  
208  
209  
210  
211  
212  
213  
214  
215  
216  
217  
218  
219  
220  
221  
222  
223  
224  
225  
226  
227  
228  
229

**Fig. 1. Resistance of B.1.1.529 to neutralization by sera.** **a**, Unrooted phylogenetic tree of B.1.1.529 with other major SARS-CoV-2 variants. **b**, Key spike mutations found in the viruses isolated in the major lineage of B.1.1.529 are denoted. **c**, Neutralization of D614G and B.1.1.529 pseudoviruses by convalescent patient sera. **d**, Neutralization of D614G and B.1.1.529 pseudoviruses by vaccinee sera. Within the four standard vaccination groups, individuals that were vaccinated without documented infection are denoted as circles and individuals that were both vaccinated and infected are denoted as triangles. Within the boosted group, Moderna vaccinees are denoted as squares and Pfizer vaccinees are denoted as diamonds. **e**, Neutralization of authentic D614G and B.1.1.529 viruses by vaccinee sera. Moderna vaccinees are denoted as squares and Pfizer vaccinees are denoted as diamonds. Data represent one of two independent experiments. For all panels, values above the symbols denote geometric mean titer and the numbers in parentheses denote the number of samples above the limit of detection. *P* values were determined by using a Wilcoxon matched-pairs signed-rank test (two-tailed).

**Fig. 2**



230 **Fig. 2. Resistance of B.1.1.529 to neutralization by monoclonal antibodies.** **a**, Footprints of  
231 RBD-directed antibodies, with mutations within B.1.1.529 highlighted in cyan. Approved or  
232 authorized antibodies are bolded. The receptor binding motif (RBM) residues are highlighted in  
233 yellow. **b**, Footprints of NTD-directed antibodies, with mutations within B.1.1.529 highlighted in  
234 cyan. The NTD supersite residues are highlighted in light pink. **c**, Neutralization of D614G and  
235 B.1.1.529 pseudoviruses by RBD-directed and NTD-directed mAbs. **d**, Neutralization D614G and  
236 B.1.1.529+R346K pseudoviruses by RBD-directed and NTD-directed mAbs. Data represent one  
237 of two independent experiments.

238  
239  
240  
241  
242  
243  
244  
245  
246  
247  
248  
249  
250  
251  
252  
253  
254  
255  
256  
257  
258  
259

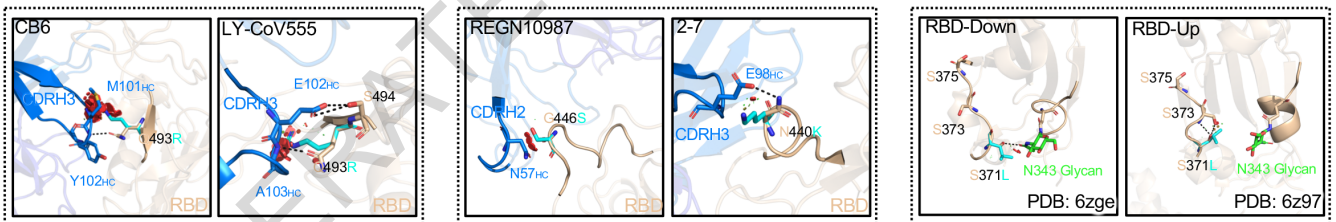
Fig. 3

a

Fold change in IC50 compared with WT	RBD mAbs																	NTD mAbs	
	Class 1				Class 2				Class 3				Class 4					4-18	5-7
	CB6	Brii-196	1-20	910-30	REGN10933	COV2-2196	LY-CoV555	2-15	REGN10987	COV2-2130	S309	2-7	Brii-198	ADG-2	DH1047	10-40	S2X259		
B.1.1.529	<-1000	-134	<-338	<-159	<-1000	-140	<-1000	<-1000	<-1000	-390	-2.5	-231	2.2	-43	-124	-11	-35	-125	-30
B.1.1.529 + R346K	<-761	-97	<-338	<-159	<-1000	-89	<-1000	<-1000	<-1000	<-988	-2.4	-109	<-32	-51	-167	-32	-16	-125	-33
A67V	1.1	1.0	-1.1	1.4	1.1	-1.0	1.1	1.1	1.1	1.2	-1.4	-1.1	-1.2	1.3	-1.3	-1.1	1.0	-1.6	-1.1
Del69-70	-1.4	-1.4	-1.6	-1.1	-1.8	-1.5	-1.4	-1.4	-1.7	-1.4	-2.2	-1.9	-2.3	-1.4	-3.3	-1.7	-1.3	-2.6	-9.4
T95I	-1.4	-2.0	-1.8	-1.7	-1.5	-1.6	-1.5	1.1	-2.0	-1.1	-2.3	-3.4	1.3	-2.5	-3.4	-1.9	-2.2	1.0	-9.5
G142D	-1.3	-1.4	-1.6	1.0	-1.6	-1.6	-1.7	-1.6	-1.9	-1.5	-2.9	-2.9	-1.5	-1.4	-2.8	-1.4	-1.5	<-125	-263
Del143-145	1.3	1.0	-1.2	1.4	1.3	1.6	1.3	1.5	1.1	-1.1	-1.9	1.2	-1.3	1.2	-2.0	-1.2	-1.2	<-125	-29
Del211	-2.4	-2.1	-1.6	-2.1	-1.5	-1.5	-1.4	-1.2	1.2	-1.2	-1.2	-1.3	-1.1	-1.9	-2.4	-1.6	-2.3	1.2	-9.1
L212I	-1.3	-1.8	-1.3	-1.6	-1.4	-1.4	-1.6	-1.3	-1.3	-1.4	-2.2	-1.9	-2.2	-1.7	-3.2	-2.0	-1.9	-7.2	-2.2
Ins214EPE	-2.4	-2.4	-2.2	-2.4	-2.8	-2.7	-2.3	-4.3	-3.0	-2.2	-3.0	-6.2	-2.7	-3.1	-2.9	-1.9	-3.3	-7.1	-15
G339D	-1.7	-1.6	-1.7	-1.4	-2.2	-1.7	-1.5	-1.4	-1.8	-1.6	-4.0	-1.9	-3.9	-1.6	-2.2	-1.5	-3.2	-4.5	-3.0
(R346K)	-1.5	-1.2	-1.3	1.0	-1.5	-1.3	-1.3	-1.4	-1.6	-2.9	-1.4	-1.0	-21	-1.1	-1.9	-1.2	-1.4	-1.4	-2.3
S371L	-19	-18	-15	-22	-10	-4.1	-2.9	-1.4	-25	-1.4	-12	-12	-17	-18	-49	-59	-23	-1.8	1.1
S373P	-1.9	-2.1	-1.6	-1.4	-1.9	-2.1	-2.0	-1.4	-1.9	-1.3	-2.3	-1.8	-2.5	-2.2	-5.1	-5.0	-2.8	-8.2	-5.0
S375F	1.7	1.6	1.6	1.5	2.1	1.9	1.9	2.6	1.2	1.5	-1.1	1.4	1.1	1.8	-1.8	-1.2	-1.6	-9.2	-1.6
K417N	<-761	-1.6	-2.3	<-158	-6.4	1.1	1.5	1.1	1.2	1.2	-1.8	1.5	-1.0	-1.1	-1.9	-1.5	-1.8	-5.3	-2.8
N440K	-1.4	-1.4	-1.6	-1.2	-1.7	-1.4	-1.4	-1.6	-246	-1.5	-2.3	-18	-1.6	1.1	-2.0	-1.3	-1.5	-4.3	-2.8
G446S	1.3	1.1	-1.1	1.2	-1.6	-1.1	-1.6	-3.0	-574	-3.7	-1.7	-50	-1.4	-1.6	-2.2	-1.4	-2.2	-3.9	-2.4
S477N	-1.8	-1.8	-1.7	-1.7	-2.4	-1.5	-1.5	-1.7	-2.9	-1.6	-1.9	-4.4	-2.4	-1.5	-2.3	-1.6	-2.2	-17	-5.1
T478K	1.2	1.1	1.4	1.6	1.3	-1.5	-1.4	-1.2	-1.6	1.1	-1.8	-2.6	-1.6	-1.2	-2.8	-1.3	-2.3	-3.3	-2.3
E484A	-2.8	-1.7	-1.8	-1.2	-4.8	-4.9	<-1000	<-1000	-1.6	-1.4	-1.4	-2.7	-1.9	-1.6	-1.5	-1.9	-1.9	-5.7	-2.9
Q493R	-16	-7.3	-3.2	2.9	-42	-4.2	<-1000	-705	-1.4	-1.1	-1.2	-1.9	-2.0	-1.6	-1.6	-1.6	-1.5	-4.0	-1.3
G496S	-1.3	1.3	1.1	1.1	1.0	1.1	1.0	-9.3	-6.2	-1.3	-1.4	1.4	-1.2	-1.2	-1.6	-1.1	-1.6	-2.6	-1.6
Q498R	-1.7	-1.2	1.1	1.4	-1.5	-1.1	-1.4	-1.0	-1.6	-1.4	-1.3	1.1	-1.2	2.4	-1.3	-1.2	-1.3	-1.5	-1.8
N501Y	-9.8	-1.2	-8.4	-16	-1.4	-1.5	-1.6	-1.2	-1.2	-1.1	-1.8	-1.5	-2.7	-1.8	-2.5	-1.9	-1.9	-20	-3.9
Y505H	-1.2	1.2	-1.3	-9.6	1.1	1.0	1.0	1.1	1.4	1.0	-1.4	1.7	1.1	1.3	-1.4	1.0	-1.2	-1.2	-1.1
T547K	-1.9	-2.0	-2.0	-1.9	-1.7	-1.3	-1.6	-1.7	-2.7	-1.6	-1.6	-4.3	-1.9	-1.7	-2.6	-1.5	-1.9	-2.7	-2.7
H655Y	-2.7	-3.1	-3.5	-2.7	-3.1	-2.0	-2.2	-8.6	-8.8	-1.7	-2.3	-13	-2.4	-2.1	-3.9	-3.3	-3.9	-23	-5.3
N679K	1.0	1.2	1.1	1.1	-1.1	-1.2	-1.2	-1.2	-1.9	-1.1	-1.3	-1.8	-1.7	-1.4	-2.4	-1.7	-1.7	-2.1	-2.7
P681H	-2.3	-2.1	-2.1	1.0	-2.4	-1.8	-2.2	-1.5	-1.5	-1.0	-1.6	-1.9	-1.5	-1.3	-2.3	-1.3	-1.3	-2.3	-2.4
N764K	-1.1	-1.5	-1.3	-1.1	-1.4	-1.4	-1.4	-2.1	-2.5	-1.5	-2.2	-4.3	-1.3	-1.4	-3.3	-2.1	-2.4	-2.3	-2.1
D769Y	1.3	1.1	1.0	1.2	-1.5	-1.0	-1.4	-1.4	-2.0	-1.3	-1.9	-2.5	-1.3	-1.1	-1.7	-1.2	-1.4	-3.1	-2.5
N856K	-10	-2.8	-1.3	-12	-2.2	-3.0	-1.1	-1.0	-1.4	-1.1	-1.2	-1.3	-2.3	-1.8	-4.4	-2.1	-2.5	-1.6	-1.9
Q954H	2.7	1.9	1.5	2.6	1.2	1.0	1.2	1.1	-1.1	1.2	-1.2	-1.4	-1.1	-1.1	-2.5	-1.0	-1.1	-2.3	-2.9
N969K	-5.4	-1.6	-1.1	-4.5	-1.3	-1.8	-1.1	-1.3	-1.6	-1.1	-1.4	-2.4	-1.4	-1.1	-2.3	-2.0	-2.4	-2.5	-2.0
L981F	3.2	3.3	2.1	4.6	2.4	2.5	2.2	1.9	1.3	2.5	-1.0	-1.5	8.6	2.8	1.1	2.0	2.1	-1.3	-1.5

Legend: >3 <-3 <-10 <-100

b



260 **Fig. 3. Impact of individual mutations within B.1.1.529 against monoclonal antibodies. a,**  
261 Neutralization of pseudoviruses harboring single mutations found within B.1.1.529 by a panel of  
262 19 monoclonal antibodies. Fold change relative to neutralization of D614G is denoted, with  
263 resistance colored red and sensitization colored green. **b,** Modeling of critical mutations in  
264 B.1.1.529 that affect antibody neutralization.

265  
266  
267  
268  
269  
270  
271  
272  
273  
274  
275  
276  
277  
278  
279  
280  
281  
282  
283  
284  
285  
286  
287  
288

Fig. 4

Fold change in IC50 compared with WT	RBD mAbs																	NTD mAbs	
	Class 1				Class 2				Class 3					Class 4				4-18	5-7
	CB6	Brii-196	1-20	910-30	REGN10933	COV2-2196	LY-CoV555	2-15	REGN10987	COV2-2130	S309	2-7	Brii-198	ADG-2	DH1047	10-40	S2X259		
B.1.1.7	-8.8	2.6	-5.2	-15	1.6	1.8	1.6	2.2	2.9	1.7	1.1	2.3	4.1	1.7	2.2	1.4	1.4	-5.1	-4.0
B.1.526	-1.0	1.1	-1.1	2.5	-4.5	-2.1	-590	-1329	1.8	1.2	2.9	1.8	-1.1	1.5	2.9	-2.2	1.4	4.5	-2.5
B.1.429	3.0	2.3	1.4	2.5	2.5	2.8	-590	-4.6	1.6	1.1	1.9	1.6	-2.4	2.0	2.9	1.3	3.3	-39	-59
B.1.617.2	2.1	1.2	-1.1	2.5	1.2	1.4	-590	-10	-1.8	-1.7	1.2	-1.1	-8.9	1.0	1.4	-1.8	-1.4	-39	-74
P.1	-196	2.2	-16	-60	-121	-2.0	-590	-1329	1.9	1.1	1.1	1.2	1.8	-1.0	3.0	-2.2	1.2	-39	-74
B.1.351	-196	2.0	-40	-60	-78	-2.5	-590	-1329	1.5	1.5	1.2	1.9	-1.5	1.0	3.0	-2.9	1.2	-39	-8.4
B.1.1.529	<-1000	-134	<-338	<-159	<-1000	-140	<-1000	<-1000	<-1000	-390	-2.5	-231	2.2	-43	-124	-11	-35	-125	-30
B.1.1.529 + R346K	<-761	-97	<-338	<-159	<-1000	-89	<-1000	<-1000	<-1000	<-988	-2.4	-109	<-32	-51	-167	-32	-16	-125	-33

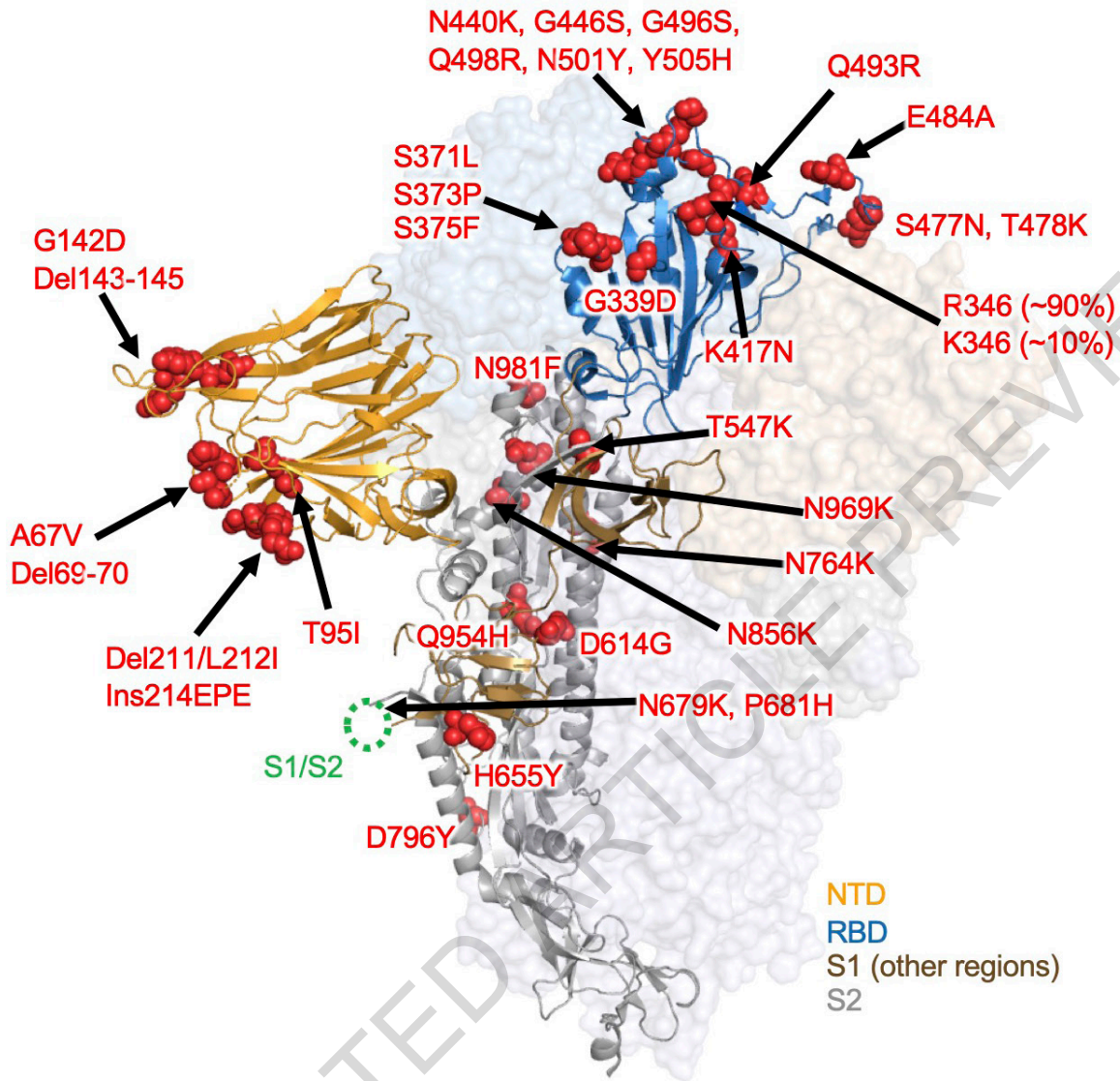
Legend: >3 <-3 <-10 <-100

ACCELERATED ARTICLE PREVIEW

289 **Fig. 4. Evolution of antibody resistance across SARS-CoV-2 variants.** Neutralization of SARS-  
290 CoV-2 variant pseudoviruses by a panel of 19 monoclonal antibodies. Fold change relative to  
291 neutralization of D614G is denoted.

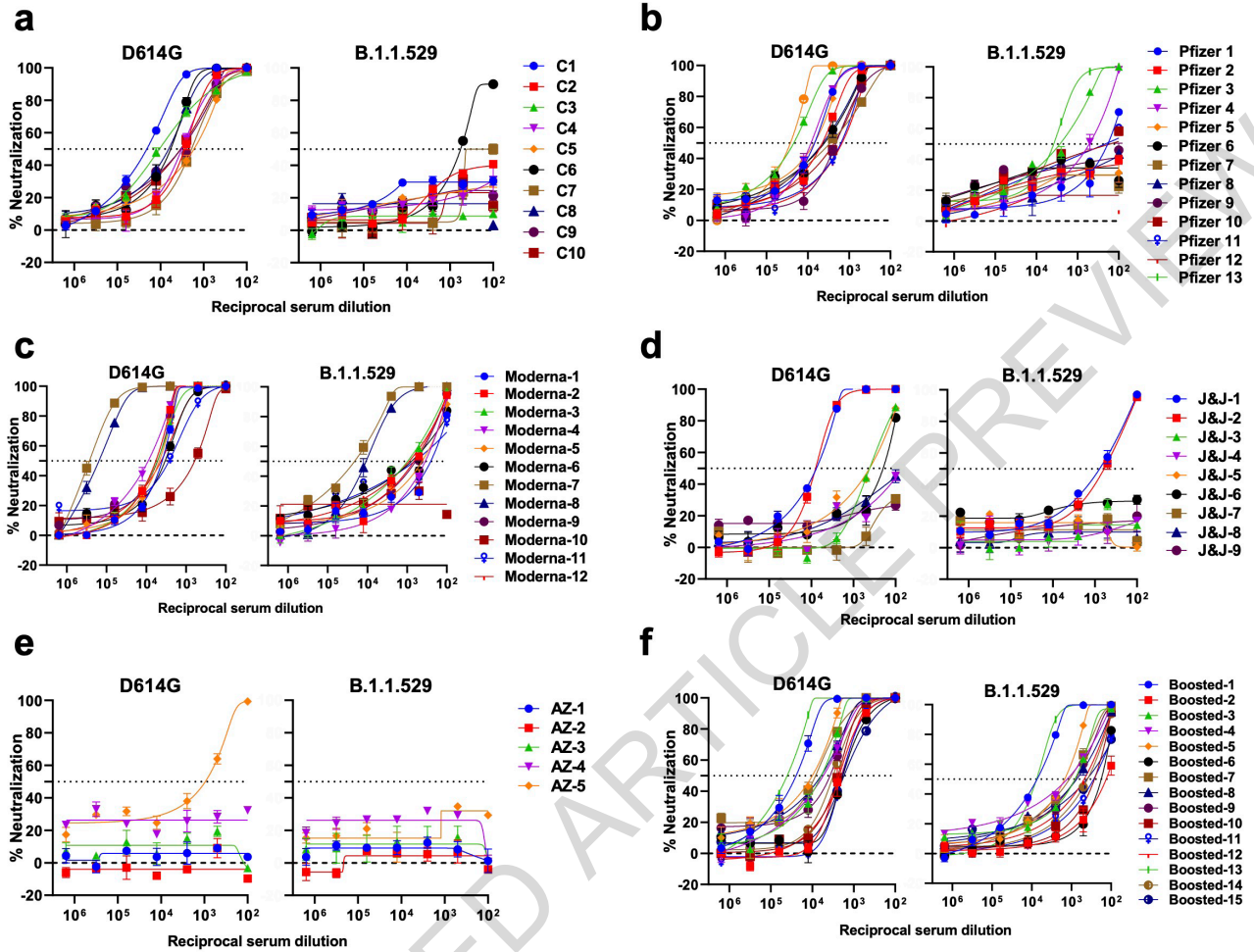
292  
293  
294  
295  
296  
297  
298  
299  
300  
301  
302  
303  
304  
305  
306  
307  
308  
309  
310  
311  
312  
313  
314  
315  
316  
317  
318  
319

Extended Data Fig. 1



320 **Extended Data Fig. 1. Mutations within B.1.1.529 denoted on the full SARS-CoV-2 spike**  
321 **trimer.** The SARS-CoV-2 spike structure was downloaded from PDB 6ZGE.

322  
323  
324  
325  
326  
327  
328  
329  
330  
331  
332  
333  
334  
335  
336  
337  
338  
339  
340  
341  
342  
343  
344  
345  
346  
347  
348  
349  
350

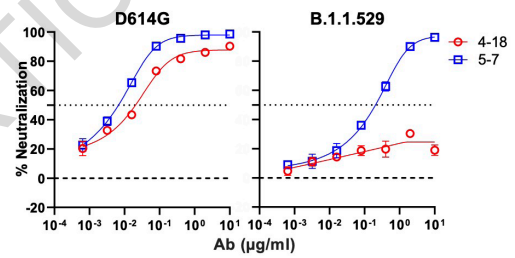
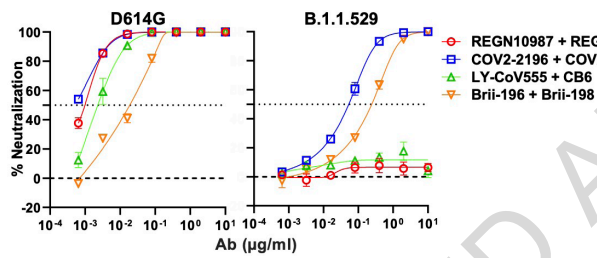
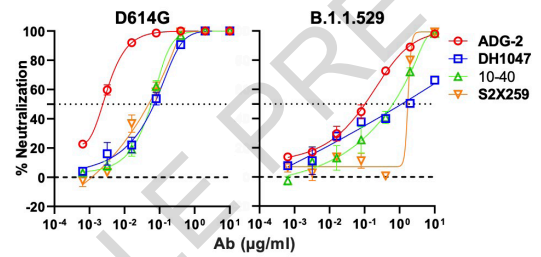
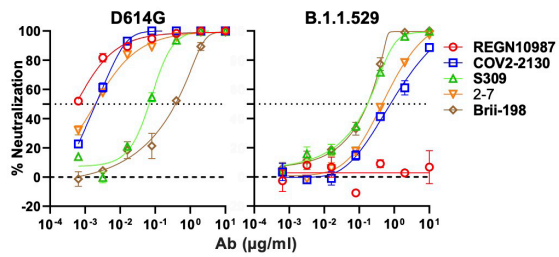
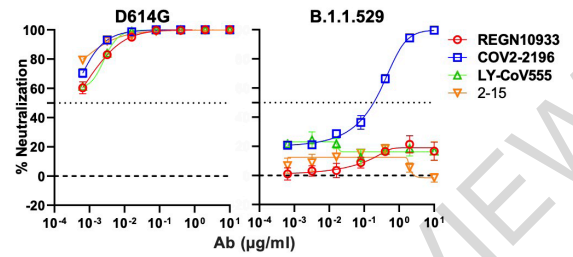
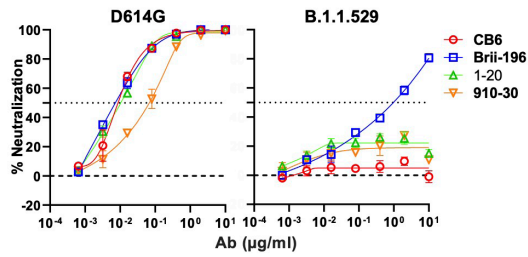


ACCELERATED ARTICLE PREVIEW

351 **Extended Data Fig. 2. Individual neutralization curves for pseudovirus neutralization assays**  
352 **by serum.** Neutralization by **a**, convalescent sera. **b**, Pfizer (BNT162b2) vaccinee sera. **c**, Moderna  
353 (mRNA-1273) vaccinee sera. **d**, J&J (Ad26.COV2.S) vaccinee sera. **e**, AstraZeneca (ChAdOx1  
354 nCoV-19) vaccinee sera. **f**, boosted (three homologous BNT162b2 or mRNA-1273 vaccinations)  
355 vaccinee sera. Error bars denote mean  $\pm$  standard error of the mean (SEM) for three technical  
356 replicates.

357  
358  
359  
360  
361  
362  
363  
364  
365  
366  
367  
368  
369  
370  
371  
372  
373  
374  
375  
376  
377  
378  
379  
380  
381

# Extended Data Fig. 3

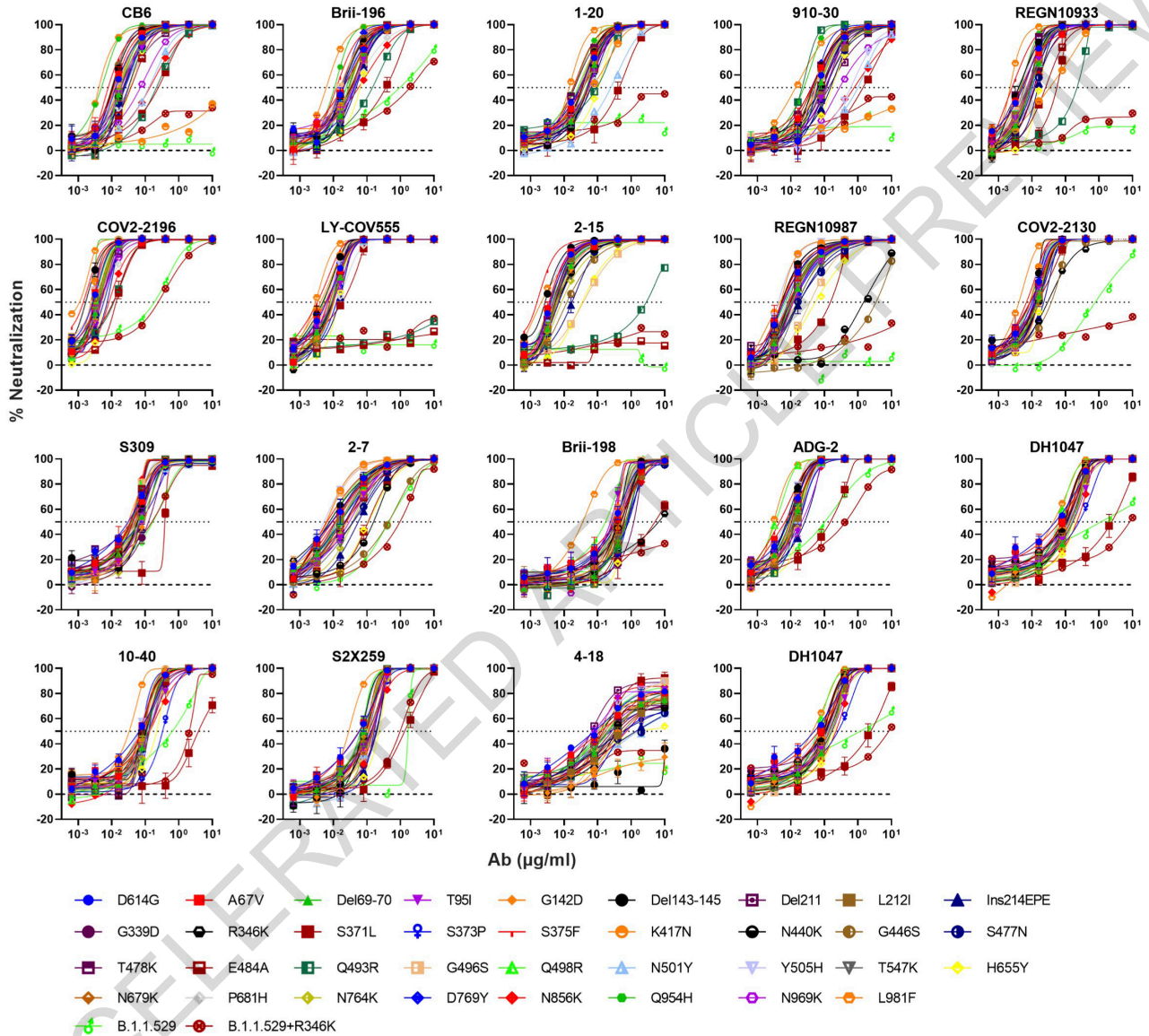


ACCELERATED ARTICLE PREVIEW

382 **Extended Data Fig. 3. Individual neutralization curves for pseudovirus neutralization assays**  
383 **by monoclonal antibodies.** Error bars denote mean  $\pm$  standard error of the mean (SEM) for three  
384 technical replicates.

385  
386  
387  
388  
389  
390  
391  
392  
393  
394  
395  
396  
397  
398  
399  
400  
401  
402  
403  
404  
405  
406  
407  
408  
409  
410  
411

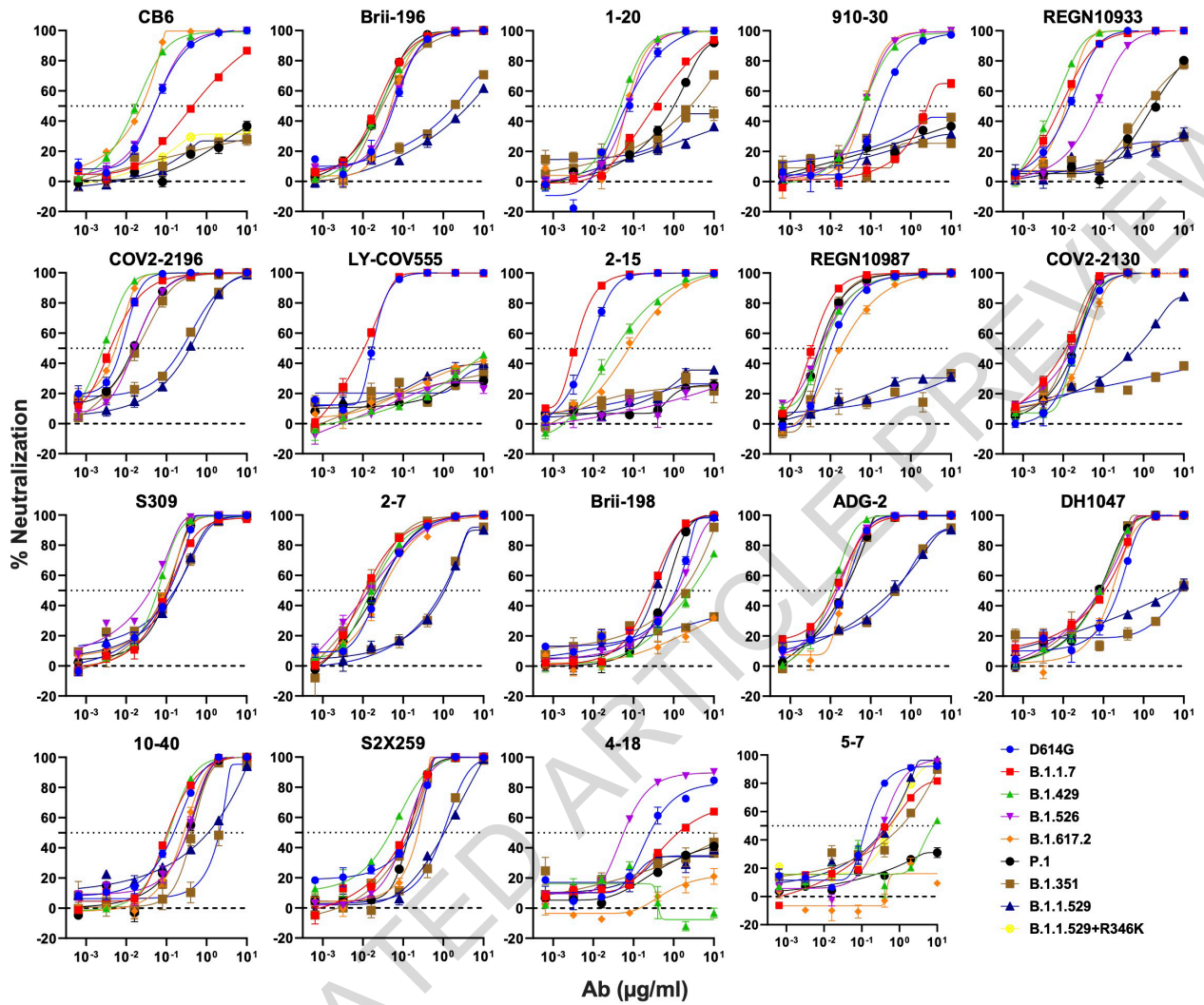
# Extended Data Fig. 4



412 **Extended Data Fig. 4. Individual neutralization curves for pseudovirus neutralization assays**  
413 **by monoclonal antibodies against individual SARS-CoV-2 mutations.** Error bars denote mean  
414  $\pm$  standard error of the mean (SEM) for three technical replicates.

415  
416  
417  
418  
419  
420  
421  
422  
423  
424  
425  
426  
427  
428  
429  
430  
431  
432  
433  
434  
435  
436  
437  
438  
439  
440  
441

Extended Data Fig. 5



ACCELERATED

442 **Extended Data Fig. 5. Individual neutralization curves for pseudovirus neutralization assays**  
443 **by monoclonal antibodies against SARS-CoV-2 variants.** Error bars denote mean  $\pm$  standard  
444 error of the mean (SEM) for three technical replicates.

445  
446  
447  
448  
449  
450  
451  
452  
453  
454  
455  
456  
457  
458  
459  
460  
461  
462  
463  
464  
465  
466  
467  
468  
469  
470  
471

## Extended Data Table 1

Convalescent Sample	Days post-symptoms	Age	Gender
C1	18	57	Female
C2	25	51	Male
C3	29	71	Female
C4	32	50	Male
C5	35	59	Male
C6	120	56	Male
C7	105	54	Female
C8	77	51	Female
C9	18	79	Male
C10	9	45	Male

ACCELERATED ARTICLE PREVIEW

472 **Extended Data Table 1. Demographics and vaccination information for serum samples from**  
473 **convalescent patients used in this study.**

474  
475  
476  
477  
478  
479  
480  
481  
482  
483  
484  
485  
486  
487  
488  
489  
490  
491  
492  
493  
494  
495  
496  
497  
498  
499  
500  
501

## Extended Data Table 2

Vaccine Sample	Vaccine type	Days post-vaccination (after last dose)	Documented COVID Infection	Age	Gender
Moderna vaccinee #1	mRNA-1273	31	No	72	Male
Moderna vaccinee #2	mRNA-1273	19	No	38	Female
Moderna vaccinee #3	mRNA-1273	6	No	42	Male
Moderna vaccinee #4	mRNA-1273	81	No	40	Female
Moderna vaccinee #5	mRNA-1273	123	No	40	Female
Moderna vaccinee #6	mRNA-1273	177	No	40	Female
Moderna vaccinee #7	mRNA-1273	29	No	57	Female
Moderna vaccinee #8	mRNA-1273	74	No	57	Female
Moderna vaccinee #9	mRNA-1273	32	No	66	Female
Moderna vaccinee #10	mRNA-1273	72	No	63	Male
Moderna vaccinee #11	mRNA-1273	74	No	68	Female
Moderna vaccinee #12	mRNA-1273	58	No	46	Female
Pfizer vaccinee #1	BNT162b2	21	No	62	Male
Pfizer vaccinee #2	BNT162b2	36	No	62	Male
Pfizer vaccinee #3	BNT162b2	26	No	38	Male
Pfizer vaccinee #4	BNT162b2	66	No	38	Male
Pfizer vaccinee #5	BNT162b2	22	No	57	Female
Pfizer vaccinee #6	BNT162b2	61	No	57	Female
Pfizer vaccinee #7	BNT162b2	20	No	55	Male
Pfizer vaccinee #8	BNT162b2	16	No	64	Female
Pfizer vaccinee #9	BNT162b2	32	No	68	Male
Pfizer vaccinee #10	BNT162b2	20	No	35	Male
Pfizer vaccinee #11	BNT162b2	15	No	48	Female
Pfizer vaccinee #12	BNT162b2	21	No	45	Male
Pfizer vaccinee #13	BNT162b2	213	Yes	66	Male
J&J vaccinee #1 (BEI Cat. #NRH-10818)	Ad26.COV2.S	55	Yes	50	Female
J&J vaccinee #2 (BEI Cat. #NRH-10819)	Ad26.COV2.S	61	Yes	50	Female
J&J vaccinee #3 (BEI Cat. #NRH-10835)	Ad26.COV2.S	186	Unknown	43	Female
J&J vaccinee #4 (BEI Cat. #NRH-10845)	Ad26.COV2.S	69	Unknown	28	Female
J&J vaccinee #5 (BEI Cat. #NRH-10823)	Ad26.COV2.S	50	No	42	Female
J&J vaccinee #6 (BEI Cat. #NRH-10834)	Ad26.COV2.S	175	Unknown	43	Female
J&J vaccinee #7 (BEI Cat. #NRH-10839)	Ad26.COV2.S	39	No	47	Male
J&J vaccinee #8 (BEI Cat. #NRH-10844)	Ad26.COV2.S	60	Unknown	28	Female
J&J vaccinee #9 (BEI Cat. #NRH-10824)	Ad26.COV2.S	51	No	43	Male
AZ vaccinee #1 (BEI Cat. #NRH-10817)	ChAdOx1 nCoV-19	158	Unknown	73	Male
AZ vaccinee #2 (BEI Cat. #NRH-10814)	ChAdOx1 nCoV-19	152	Unknown	36	Female
AZ vaccinee #3 (BEI Cat. #NRH-10815)	ChAdOx1 nCoV-19	159	Unknown	36	Female
AZ vaccinee #4 (BEI Cat. #NRH-10811)	ChAdOx1 nCoV-19	142	Yes	26	Female
AZ vaccinee #5 (BEI Cat. #NRH-3083)	ChAdOx1 nCoV-19	91	Unknown	56	Female
Boosted sera #1	mRNA-1273/mRNA-1273	28	No	66	Female
Boosted sera #2	BNT162b2/BNT162b2	30	No	68	Male
Boosted sera #3	BNT162b2/BNT162b2	14	No	64	Female
Boosted sera #4	BNT162b2/BNT162b2	34	No	55	Male
Boosted sera #5	BNT162b2/BNT162b2	34	No	45	Male
Boosted sera #6	BNT162b2/BNT162b2	15	No	50	Female
Boosted sera #7	BNT162b2/BNT162b2	15	No	48	Female
Boosted sera #8	BNT162b2/BNT162b2	29	No	71	Male
Boosted sera #9	BNT162b2/BNT162b2	90	No	59	Male
Boosted sera #10	BNT162b2/BNT162b2	33	No	45	Male
Boosted sera #11	BNT162b2/BNT162b2	87	No	66	Female
Boosted sera #12	BNT162b2/BNT162b2	84	No	26	Male
Boosted sera #13	mRNA-1273/mRNA-1273	23	No	28	Female
Boosted sera #14	BNT162b2/BNT162b2	14	No	78	Male
Boosted sera #15	BNT162b2/BNT162b2	14	No	75	Female

502 **Extended Data Table 2. Demographics and vaccination information for serum samples from**  
503 **vaccinated individuals used in this study.**

504  
505  
506  
507  
508  
509  
510  
511  
512  
513  
514  
515  
516  
517  
518  
519  
520  
521  
522  
523  
524  
525  
526  
527  
528  
529  
530  
531  
532

### Extended Data Table 3

Oligo name	Targeted mutations	Oligo sequence
O_single_mutant1	A67V	ATGTGACCTGGTTCCATGTGATCCATGTGTCTGGCACCAATGGCACC
O_single_mutant2	Del69-70	CTGGTTCCATGCCATCTCTGGCACCAATGGCAC
O_single_mutant3	T95I	CTTTGCCAGCATCGAGAAGAGCAACATCATC
O_single_mutant4	Del143-145	TGTAATGACCCATTCTGGGACACAAGAACAACAAGTCTGGATG
O_single_mutant5	G142D	GTAATGACCCATTCTGGACGTCTACTACCACAAG
O_single_mutant6	Del211	ACACACACCAATCCTGGTGAGGGACCTG
O_single_mutant7	L212I	CACACCAATCAACATCGTGAGGGACCTGCC
O_single_mutant8	Ins214EPE	ACCAATCAACCTGGTGAGGGAGCCCGAGGACCTGCCACAGGGCTT
O_single_mutant9	G339D	CTGTGTCCATTTGACGAGGTGTTCAATGCCAC
O_single_mutant10	R346K	TGTTCAATGCCACCAAGTTTGCCTCTGTCTATGCCTG
O_single_mutant11	S371F	CTCTGTGCTCTACAACCTTTCCTCCTTCAGCAC
O_single_mutant12	S371L	CTCTGTGCTCTACAACCTGGCCTCCTTCAGCAC
O_single_mutant13	S373P	CTCTACAACCTGCCCTTCAGCACCTTCAAG
O_single_mutant14	S375F	CAACTCTGCCTCCTTCTTCACTTCAAGTGTATGG
O_single_mutant15	K417N	CCCCTGGACAACAGGCAACATTGCTGACTACAACCTACAACTGC
O_single_mutant16	N440K	CCTGGAACAGCAACAAGCTGGACAGCAAGGTG
O_single_mutant17	G446S	GGACAGCAAGGTGAGCGGCAACTACAACCTAC
O_single_mutant18	S477N	GATTTACCAGGCTGGCAACACACCATGTAAATG
O_single_mutant19	T478K	CAGGCTGGCAGCAAGCCATGTAATGGAGTGGA
O_single_mutant20	E484A	GTAATGGAGTGCCCGGCTTCAACTGTTAC
O_single_mutant21	Q493R	GTTACTTTCCACTCAGATCCTATGGCTTCCAAC
O_single_mutant22	G496S	CACTCCAATCCTATAGCTTCCAACCAACCAATG
O_single_mutant23	Q498R	CAATCCTATGGCTTCAGACCAACCAATGGAGTGGG
O_single_mutant24	N501Y	CTTCCAACCAACCTACGGAGTGGGCTACCAACC
O_single_mutant25	Y505H	AATGGAGTGGGCCACCAACCATAACAGG
O_single_mutant26	T547K	CTTCAATGGACTGAAGGGCACAGGAGTGCTGAC
O_single_mutant27	H655Y	CTGATTGGAGCAGAGTACGTGAACAACCTCCTATG
O_single_mutant28	N679K	CCAGACCCAGACCAAGAGCCCAAGGAGGGCA
O_single_mutant29	P681H	CCCAGACCAACAGCAGAAGGAGGGCAAGGTCTGTGGC
O_single_mutant30	N764K	GTACCCAACCTAAGAGGGCTCTGACAGGC
O_single_mutant31	D769Y	GACACCTCAATCAAGTACTTTGGAGGCTTC
O_single_mutant32	N856K	GTGCCCAGAAGTTCAAGGGACTGACAGTGCTG
O_single_mutant33	Q954H	CAAGATGTGGTGAACCACAATGCCAGGCTCTG
O_single_mutant34	N969K	GCAACTTTCCAGCAAGTTTGGAGCCATCTCCTC
O_single_mutant35	L981F	GTGCTGAATGACATCTTCCAGCAGACTGGACAAGGTGGAGG
O_multiple_oligo1	A67V, Del69-70	TGGTTCCATGTGATCTCTGGCACCAATGG
O_multiple_oligo2	T95I	CTTTGCCAGCATCGAGAAGAGCAAC
O_multiple_oligo3	G142D, Del143-145	GACCCATTCTGGACCACAAGAACAACAAGTC
O_multiple_oligo4	L212I, Ins214EPE	CACACACCAATCATCTGTGAGGGAGCCCGAGGACCTGCCACAGGGCTTC
O_multiple_oligo5	G339D	TGTGCTCATTTGACGAGGTGTTCAATG
O_multiple_oligo6	S371L, S373P, S375F	TGTGCTCTACAACCTGGCCCCCTTCTTCACTTCAAGTGTATG
O_multiple_oligo7	K417N	GGACAACAGGCAACATTGCTGACTACA
O_multiple_oligo8	N440K, G446S	GCAACAAGCTGGACAGCAAGGTGAGCGGCAACTACAA
O_multiple_oligo9	S477N, T478K, E484A	ACCAGGCTGGCAACAAGCCATGTAATGGAGTGGCCGGCTTCAACTGT
O_multiple_oligo10	Q493R, G496S, Q498R, N501Y, Y505H	TACTTTCCACTCAGATCCTATAGCTTCCAGACCAACCTACGGAGTGGGCCACCAACCATAACAGG
O_multiple_oligo11	T547K	GGACTGAAGGGCACAGGAG
O_multiple_oligo12	D614G	CTCTACCAGGGCGTGAACCTGAC
O_multiple_oligo13	H655Y	TTGGAGCAGAGTACGTGAACAACCT
O_multiple_oligo14	N679K, P681H	CAGACCAAGAGCCACAGGAGGGCAAGG
O_multiple_oligo15	N764K	CCAACCTAAGAGGGCTCTGACAG
O_multiple_oligo16	D796Y	CCTCCAATCAAGTACTTTGGAGGCTTC
O_multiple_oligo17	N856K	CAGAAGTTCAAGGGACTGACAGTGCTG
O_multiple_oligo18	Q954H	GTGGTGAACCACAATGCCAGGCTC
O_multiple_oligo19	N969K	AACTTTCCAGCAAGTTTGGAGCCATCTCCTC
O_multiple_oligo20	L981F	AATGACATCTTCCAGCAGACTGGACAAGGTGGAGGCTGAGGTCCAGATTG

533 **Extended Data Table 3. Oligos used to construct spike expression plasmids.**

534

ACCELERATED ARTICLE PREVIEW

535 **References**

536

- 537 1 Shu, Y. & McCauley, J. GISAID: Global initiative on sharing all influenza data - from  
538 vision to reality. *Euro Surveill* **22**, doi:10.2807/1560-7917.ES.2017.22.13.30494 (2017).
- 539 2 Grabowski, F., Kochańczyk, M. & Lipniacki, T. Omicron strain spreads with the  
540 doubling time of 3.2—3.6 days in South Africa province of Gauteng that achieved herd  
541 immunity to Delta variant. *medRxiv*, doi:<https://doi.org/10.1101/2021.12.08.21267494>  
542 (2021).
- 543 3 Scott, L. *et al.* Track Omicron's spread with molecular data. *Science*, eabn4543,  
544 doi:10.1126/science.abn4543 (2021).
- 545 4 Wang, P. *et al.* Antibody resistance of SARS-CoV-2 variants B.1.351 and B.1.1.7.  
546 *Nature* **593**, 130-135, doi:10.1038/s41586-021-03398-2 (2021).
- 547 5 Abu-Raddad, L. J., Chemaitelly, H., Butt, A. A. & National Study Group for, C.-V.  
548 Effectiveness of the BNT162b2 Covid-19 Vaccine against the B.1.1.7 and B.1.351  
549 Variants. *N Engl J Med* **385**, 187-189, doi:10.1056/NEJMc2104974 (2021).
- 550 6 Madhi, S. A. *et al.* Efficacy of the ChAdOx1 nCoV-19 Covid-19 Vaccine against the  
551 B.1.351 Variant. *N Engl J Med* **384**, 1885-1898, doi:10.1056/NEJMoa2102214 (2021).
- 552 7 Sadoff, J. *et al.* Safety and Efficacy of Single-Dose Ad26.COV2.S Vaccine against  
553 Covid-19. *N Engl J Med* **384**, 2187-2201, doi:10.1056/NEJMoa2101544 (2021).
- 554 8 Davies, N. G. *et al.* Estimated transmissibility and impact of SARS-CoV-2 lineage  
555 B.1.1.7 in England. *Science* **372**, doi:10.1126/science.abg3055 (2021).
- 556 9 Mlcochova, P. *et al.* SARS-CoV-2 B.1.617.2 Delta variant replication and immune  
557 evasion. *Nature* **599**, 114-119, doi:10.1038/s41586-021-03944-y (2021).
- 558 10 Hadfield, J. *et al.* Nextstrain: real-time tracking of pathogen evolution. *Bioinformatics* **34**,  
559 4121-4123, doi:10.1093/bioinformatics/bty407 (2018).
- 560 11 Pulliam, J. R. C. *et al.* Increased risk of SARS-CoV-2 reinfection associated with  
561 emergence of the Omicron variant in South Africa. *medRxiv*,  
562 doi:<https://doi.org/10.1101/2021.11.11.21266068> (2021).
- 563 12 Hansen, J. *et al.* Studies in humanized mice and convalescent humans yield a SARS-  
564 CoV-2 antibody cocktail. *Science* **369**, 1010-1014, doi:10.1126/science.abd0827 (2020).

- 565 13 Zost, S. J. *et al.* Potently neutralizing and protective human antibodies against SARS-  
566 CoV-2. *Nature* **584**, 443-449, doi:10.1038/s41586-020-2548-6 (2020).
- 567 14 Jones, B. E. *et al.* The neutralizing antibody, LY-CoV555, protects against SARS-CoV-2  
568 infection in nonhuman primates. *Sci Transl Med* **13**, doi:10.1126/scitranslmed.abf1906  
569 (2021).
- 570 15 Shi, R. *et al.* A human neutralizing antibody targets the receptor-binding site of SARS-  
571 CoV-2. *Nature* **584**, 120-124, doi:10.1038/s41586-020-2381-y (2020).
- 572 16 Ju, B. *et al.* Human neutralizing antibodies elicited by SARS-CoV-2 infection. *Nature*  
573 **584**, 115-119, doi:10.1038/s41586-020-2380-z (2020).
- 574 17 Pinto, D. *et al.* Cross-neutralization of SARS-CoV-2 by a human monoclonal SARS-CoV  
575 antibody. *Nature* **583**, 290-295, doi:10.1038/s41586-020-2349-y (2020).
- 576 18 Banach, B. B. *et al.* Paired heavy- and light-chain signatures contribute to potent SARS-  
577 CoV-2 neutralization in public antibody responses. *Cell Rep* **37**, 109771,  
578 doi:10.1016/j.celrep.2021.109771 (2021).
- 579 19 Rappazzo, C. G. *et al.* Broad and potent activity against SARS-like viruses by an  
580 engineered human monoclonal antibody. *Science* **371**, 823-829,  
581 doi:10.1126/science.abf4830 (2021).
- 582 20 Li, D. *et al.* In vitro and in vivo functions of SARS-CoV-2 infection-enhancing and  
583 neutralizing antibodies. *Cell* **184**, 4203-4219 e4232, doi:10.1016/j.cell.2021.06.021  
584 (2021).
- 585 21 Tortorici, M. A. *et al.* Broad sarbecovirus neutralization by a human monoclonal  
586 antibody. *Nature* **597**, 103-108, doi:10.1038/s41586-021-03817-4 (2021).
- 587 22 Liu, L. *et al.* Potent neutralizing antibodies against multiple epitopes on SARS-CoV-2  
588 spike. *Nature* **584**, 450-456, doi:10.1038/s41586-020-2571-7 (2020).
- 589 23 Cerutti, G. *et al.* Neutralizing antibody 5-7 defines a distinct site of vulnerability in  
590 SARS-CoV-2 spike N-terminal domain. *Cell Rep* **37**, 109928,  
591 doi:10.1016/j.celrep.2021.109928 (2021).
- 592 24 Liu, L. *et al.* Isolation and comparative analysis of antibodies that broadly neutralize  
593 sarbecoviruses. *bioRxiv*, doi:<https://doi.org/10.1101/2021.12.11.472236> (2021).
- 594 25 Barnes, C. O. *et al.* SARS-CoV-2 neutralizing antibody structures inform therapeutic  
595 strategies. *Nature* **588**, 682-687, doi:10.1038/s41586-020-2852-1 (2020).

- 596 26 Cerutti, G. *et al.* Potent SARS-CoV-2 neutralizing antibodies directed against spike N-  
597 terminal domain target a single supersite. *Cell Host Microbe* **29**, 819-833 e817,  
598 doi:10.1016/j.chom.2021.03.005 (2021).
- 599 27 Uriu, K. *et al.* Neutralization of the SARS-CoV-2 Mu Variant by Convalescent and  
600 Vaccine Serum. *N Engl J Med*, doi:10.1056/NEJMc2114706 (2021).
- 601 28 Starr, T. N., Greaney, A. J., Dingens, A. S. & Bloom, J. D. Complete map of SARS-CoV-  
602 2 RBD mutations that escape the monoclonal antibody LY-CoV555 and its cocktail with  
603 LY-CoV016. *Cell Rep Med* **2**, 100255, doi:10.1016/j.xcrm.2021.100255 (2021).
- 604 29 Amanat, F. *et al.* SARS-CoV-2 mRNA vaccination induces functionally diverse  
605 antibodies to NTD, RBD, and S2. *Cell* **184**, 3936-3948 e3910,  
606 doi:10.1016/j.cell.2021.06.005 (2021).
- 607 30 Annavajhala, M. K. *et al.* Emergence and expansion of SARS-CoV-2 B.1.526 after  
608 identification in New York. *Nature* **597**, 703-708, doi:10.1038/s41586-021-03908-2  
609 (2021).
- 610 31 Zhang, W. *et al.* Emergence of a Novel SARS-CoV-2 Variant in Southern California.  
611 *JAMA* **325**, 1324-1326, doi:10.1001/jama.2021.1612 (2021).
- 612 32 Faria, N. R. *et al.* Genomics and epidemiology of the P.1 SARS-CoV-2 lineage in  
613 Manaus, Brazil. *Science* **372**, 815-821, doi:10.1126/science.abh2644 (2021).
- 614 33 Tegally, H. *et al.* Detection of a SARS-CoV-2 variant of concern in South Africa. *Nature*  
615 **592**, 438-443, doi:10.1038/s41586-021-03402-9 (2021).
- 616 34 Schmidt, F. *et al.* Plasma neutralization properties of the SARS-CoV-2 Omicron variant.  
617 *medRxiv* (2021).
- 618 35 Garcia-Beltran, W. F. *et al.* mRNA-based COVID-19 vaccine boosters induce  
619 neutralizing immunity against SARS-CoV-2 Omicron variant. *medRxiv*,  
620 doi:<https://doi.org/10.1101/2021.12.14.21267755> (2021).
- 621 36 Cameroni, E. *et al.* Broadly neutralizing antibodies overcome SARS-CoV-2 Omicron  
622 antigenic shift. *bioRxiv* (2021).
- 623 37 Doria-Rose, N. A. *et al.* Booster of mRNA-1273 Vaccine Reduces SARS-CoV-2  
624 Omicron Escape from Neutralizing Antibodies. *medRxiv* (2021).
- 625 38 Planas, D. *et al.* Considerable escape of SARS-CoV-2 variant Omicron to antibody  
626 neutralization. *bioRxiv* (2021).

627 39 Andrews, N. *et al.* Effectiveness of COVID-19 vaccines against the Omicron (B.1.1.529)  
628 variant of concern. *medRxiv*, doi:<https://doi.org/10.1101/2021.12.14.21267615> (2021).  
629 40 Wroughton, L. in *The Washington Post* (2021).  
630 41 Kuhlmann, C. *et al.* Breakthrough Infections with SARS-CoV-2 Omicron Variant  
631 Despite Booster Dose of mRNA Vaccine. *SSRN*,  
632 doi:<https://dx.doi.org/10.2139/ssrn.3981711> (2021).  
633 42 Cromer, D. *et al.* Neutralising antibody titres as predictors of protection against SARS-  
634 CoV-2 variants and the impact of boosting: a meta-analysis. *Lancet Microbe*,  
635 doi:10.1016/S2666-5247(21)00267-6 (2021).  
636

ACCELERATED ARTICLE PREVIEW

637 **Methods**

638

639 **Data reporting**

640 No statistical methods were used to predetermine sample size. The experiments were not  
641 randomized and the investigators were not blinded to allocation during experiments and outcome  
642 assessment.

643

644 **Serum samples**

645 Convalescent plasma samples were obtained from patients with documented SARS-CoV-2  
646 infection. These samples were collected at the beginning of the pandemic in early 2020 at  
647 Columbia University Irving Medical Center, and therefore are assumed to be infection by the wild-  
648 type strain of SARS-CoV-2<sup>4</sup>. Sera from individuals who received two or three doses of mRNA-  
649 1273 or BNT162b2 vaccine were collected at Columbia University Irving Medical Center at least  
650 two weeks after the final dose. Sera from individuals who received one dose of Ad26.COV2.S or  
651 two doses of ChAdOx1 nCov-19 were obtained from BEI Resources. Some individuals were also  
652 infected by SARS-CoV-2 in addition to the vaccinations they received. Note that, whenever  
653 possible, we specifically chose samples with high titers against the wild-type strain of SARS-CoV-  
654 2 such that the loss in activity against B.1.1.529 could be better quantified, and therefore the titers  
655 observed here should be considered in that context. All collections were conducted under protocols  
656 reviewed and approved by the Institutional Review Board of Columbia University. All participants  
657 provided written informed consent. Additional information for the convalescent samples can be  
658 found in **Extended Data Table 1** and for vaccinee samples can be found in **Extended Data Table**  
659 **2**.

660

661 **Monoclonal antibodies**

662 Antibodies were expressed as previously described<sup>22</sup>, by synthesis of heavy chain variable (VH)  
663 and light chain variable (VL) genes (GenScript), transfection of Expi293 cells (Thermo Fisher),  
664 and affinity purification from the supernatant by rProtein A Sepharose (GE). REGN10987,  
665 REGN10933, COV2-2196, and COV2-2130 were provided by Regeneron Pharmaceuticals, Brie-  
666 196 and Brie-198 were provided by Brie Biosciences, CB6 was provided by Baoshan Zhang and  
667 Peter Kwong (NIH), and 910-30 was provided by Brandon DeKosky (MIT).

668

669 **Cell lines**

670 Expi293 cells were obtained from Thermo Fisher (Catalog #A14527), Vero E6 cells were obtained  
671 from ATCC (Catalog# CRL-1586), HEK293T cells were obtained from ATCC (Catalog# CRL-  
672 3216), and Vero-E6-TMPRSS2 cells were obtained from JCRB (Catalog# JCRB1819). Cells were  
673 purchased from authenticated vendors and morphology was confirmed visually prior to use. All  
674 cell lines tested mycoplasma negative.

675

676 **Variant SARS-CoV-2 spike plasmid construction**

677 An in-house high-throughput template-guide gene synthesis approach was used to generate spike  
678 genes with single or full mutations of B.1.1.529. Briefly, 5'-phosphorylated oligos with designed  
679 mutations were annealed to the reverse strand of the wild-type spike gene construct and extended  
680 by DNA polymerase. Extension products (forward-stranded fragments) were then ligated together  
681 by Taq DNA ligase and subsequently amplified by PCR to generate variants of interest. To verify  
682 the sequences of variants, next generation sequencing (NGS) libraries were prepared following a  
683 low-volume Nextera sequencing protocol<sup>43</sup> and sequenced on the Illumina Miseq platform (single-  
684 end mode with 50 bp R1). Raw reads were processed by Cutadapt v2.1<sup>44</sup> with default setting to  
685 remove adapters and then aligned to reference variants sequences using Bowtie2 v2.3.4<sup>45</sup> with  
686 default setting. Resulting reads alignments were then visualized in Integrative Genomics Viewer<sup>46</sup>  
687 and subjected to manual inspection to verify the fidelity of variants. Sequences of the oligos used  
688 in variants generation are provided in **Extended Data Table 3**.

689

690 **Pseudovirus production**

691 Pseudoviruses were produced in the vesicular stomatitis virus (VSV) background, in which the  
692 native glycoprotein was replaced by that of SARS-CoV-2 and its variants, as previously  
693 described<sup>24</sup>. Briefly, HEK293T cells were transfected with a spike expression construct with  
694 polyethylenimine (PEI) (1 mg/mL) and cultured overnight at 37 °C under 5% CO<sub>2</sub>, and then  
695 infected with VSV-G pseudotyped ΔG-luciferase (G\*ΔG-luciferase, Kerafast) one day post-  
696 transfection. Following 2 h of infection, cells were washed three times, changed to fresh medium,  
697 and then cultured for approximately another 24 h before supernatants were collected, centrifuged,  
698 and aliquoted to use in assays.

699

700 **Pseudovirus neutralization assay**

701 All viruses were first titrated to normalize the viral input between assays. Heat-inactivated sera or  
702 antibodies were first serially diluted in 96 well-plates in triplicate, starting at 1:100 dilution for  
703 sera and 10 µg/mL for antibodies. Viruses were then added and the virus-sample mixture was  
704 incubated at 37 °C for 1 h. Vero-E6 cells (ATCC) were then added at a density of  $3 \times 10^4$  cells per  
705 well and plates were incubated at 37 °C for approximately 10 h. Luciferase activity was quantified  
706 by using the Luciferase Assay System (Promega) according to the manufacturer's instructions  
707 using the software SoftMax Pro 7.0.2 (Molecular Devices, LLC). Neutralization curves and IC<sub>50</sub>  
708 (50% inhibitory concentration) values were derived by fitting a non-linear five-parameter dose-  
709 response curve to the data in GraphPad Prism version 9.2.

710

711 **Authentic virus isolation and propagation**

712 Authentic B.1.1.529 was isolated from a specimen from the respiratory tract of a COVID-19  
713 patient in Hong Kong by Kwok-Yung Yuen and colleagues at the Department of Microbiology,  
714 The University of Hong Kong. Isolation of wild-type SARS-CoV-2 was previously described<sup>47</sup>.  
715 Viruses were propagated in Vero-E6-TMPRSS2 cells and sequence confirmed by next-generation  
716 sequencing prior to use.

717

718 **Authentic virus neutralization assay**

719 To measure neutralization of authentic SARS-CoV-2 viruses, Vero-E6-TMPRSS2 cells were first  
720 seeded in 96 well-plates in cell culture media (Dulbecco's Modified Eagle Medium (DMEM) +  
721 10% fetal bovine serum (FBS) + 1% penicillin/streptomycin) overnight at 37 °C under 5% CO<sub>2</sub> to  
722 establish a monolayer. The following day, sera or antibodies were serially diluted in 96 well-plates  
723 in triplicate in DMEM + 2% FBS and then incubated with 0.01 MOI (multiplicity of infection) of  
724 wild-type SARS-CoV-2 or B.1.1.529 at 37 °C for 1 h. Sera were diluted from 1:100 dilution and  
725 antibodies were diluted from 10 µg/mL. Afterwards, the mixture was overlaid onto cells and  
726 further incubated at 37 °C under 5% CO<sub>2</sub> for approximately 72 h. Cytopathic effects were then  
727 scored by plaque assay in a blinded manner. Neutralization curves and IC<sub>50</sub> values were derived  
728 by fitting a non-linear five-parameter dose-response curve to the data in GraphPad Prism version  
729 9.2.

730  
731  
732  
733  
734  
735  
736  
737  
738  
739  
740  
741

**Antibody footprint analysis and RBD mutagenesis analysis**

The SARS-CoV-2 spike structure used for displaying epitope footprints and mutations within emerging strains was downloaded from PDB (PDBID: 6ZGE). The structures of antibody-spike complexes were also obtained from PDB (7L5B for 2-15, 6XDG for REGN10933 and REGN10987, 7L2E for 4-18, 7RW2 for 5-7, 7C01 for CB6, 7KMG for LY-COV555, 7CDI for Bii-196, 7KS9 for 910-30, 7LD1 for DH1047, 7RAL for S2X259, 7LSS for 2-7, and 6WPT for S309). Interface residues were identified using PISA<sup>48</sup> using default parameters. The footprint for each antibody was defined by the boundaries of all epitope residues. The border for each footprint was then optimized by ImageMagick 7.0.10-31 (<https://imagemagick.org>). PyMOL 2.3.2 was used to perform mutagenesis and to make structural plots (Schrödinger).

742 **Acknowledgements**

743 We are grateful Regeneron Pharmaceuticals, B. Zhang and P. Kwong (NIAID), and B. Dekosky  
744 (MIT) for antibodies. This study was supported by funding from the Gates Foundation, JPB  
745 Foundation, Andrew and Peggy Cherng, Samuel Yin, Carol Ludwig, David and Roger Wu,  
746 Health@InnoHK, and the National Science Foundation (MCB-2032259).

747

748 **Author contributions**

749 D.D.H. conceived this project. L.H.L., S.I., and M.W. conducted pseudovirus neutralization  
750 experiments. J.F-W.C., H.C., K.K-H.C., T.T-T.Y., C.Y., K.K-W.T., and H.C. conducted  
751 authentic virus neutralization experiments. Y.G. and Z.Z. conducted bioinformatic analyses.  
752 L.Y.L. and Y.M.H. constructed the spike expression plasmids. Y.L. managed the project. J.Y.  
753 expressed and purified antibodies. M.T.Y. and M.E.S. provided clinical samples. M.S.N. and  
754 Y.X.H. contributed to discussions. H.H.W., K-Y.Y., and D.D.H. directed and supervised the  
755 project. L.H.L., S.I., and D.D.H. analyzed the results and wrote the manuscript.

756

757 **Competing interests**

758 L.L., S.I., M.S.N., J.Y., Y.H., and D.D.H. are inventors on patent applications (WO2021236998)  
759 or provisional patent applications (63/271,627) filed by Columbia University for a number of  
760 SARS-CoV-2 neutralizing antibodies described in this manuscript. Both sets of applications are  
761 under review. D.D.H. is a co-founder of TaiMed Biologics and RenBio, consultant to WuXi  
762 Biologics and Brie Biosciences, and board director for Vicarious Surgical.

763

764 **Data availability**

765 Materials used in this study will be made available under an appropriate Materials Transfer  
766 Agreement. All the data are provided in the paper. The structures used for analysis in this study  
767 are available from PDB under IDs 6ZGE, 7L5B, 6XDG, 7L2E, 7RW2, 7C01, 7KMG, 7CDI,  
768 7KS9, 7LD1, 7RAL, 7LSS, and 6WPT.

769

770 **Additional References**

771 43 Baym, M. *et al.* Inexpensive multiplexed library preparation for megabase-sized  
772 genomes. *PLoS One* **10**, e0128036, doi:10.1371/journal.pone.0128036 (2015).

773 44 Martin, M. Cutadapt Removes Adapter Sequences From High-Throughput Sequencing  
774 Reads. *EMBnet journal* **17**, 10, doi:10.14806/ej.17.1.200 (2011).

775 45 Langmead, B. & Salzberg, S. L. Fast gapped-read alignment with Bowtie 2. *Nat Methods*  
776 **9**, 357-359, doi:10.1038/nmeth.1923 (2012).

777 46 Robinson, J. T. *et al.* Integrative genomics viewer. *Nat Biotechnol* **29**, 24-26,  
778 doi:10.1038/nbt.1754 (2011).

779 47 Chu, H. *et al.* Comparative tropism, replication kinetics, and cell damage profiling of  
780 SARS-CoV-2 and SARS-CoV with implications for clinical manifestations,  
781 transmissibility, and laboratory studies of COVID-19: an observational study. *Lancet*  
782 *Microbe* **1**, e14-e23, doi:10.1016/S2666-5247(20)30004-5 (2020).

783 48 Krissinel, E. & Henrick, K. Inference of macromolecular assemblies from crystalline  
784 state. *J Mol Biol* **372**, 774-797, doi:10.1016/j.jmb.2007.05.022 (2007).

785

## Reporting Summary

Nature Portfolio wishes to improve the reproducibility of the work that we publish. This form provides structure for consistency and transparency in reporting. For further information on Nature Portfolio policies, see our [Editorial Policies](#) and the [Editorial Policy Checklist](#).

### Statistics

For all statistical analyses, confirm that the following items are present in the figure legend, table legend, main text, or Methods section.

- |     |           |
|-----|-----------|
| n/a | Confirmed |
|-----|-----------|
- The exact sample size ( $n$ ) for each experimental group/condition, given as a discrete number and unit of measurement
  - A statement on whether measurements were taken from distinct samples or whether the same sample was measured repeatedly
  - The statistical test(s) used AND whether they are one- or two-sided  
*Only common tests should be described solely by name; describe more complex techniques in the Methods section.*
  - A description of all covariates tested
  - A description of any assumptions or corrections, such as tests of normality and adjustment for multiple comparisons
  - A full description of the statistical parameters including central tendency (e.g. means) or other basic estimates (e.g. regression coefficient) AND variation (e.g. standard deviation) or associated estimates of uncertainty (e.g. confidence intervals)
  - For null hypothesis testing, the test statistic (e.g.  $F$ ,  $t$ ,  $r$ ) with confidence intervals, effect sizes, degrees of freedom and  $P$  value noted  
*Give  $P$  values as exact values whenever suitable.*
  - For Bayesian analysis, information on the choice of priors and Markov chain Monte Carlo settings
  - For hierarchical and complex designs, identification of the appropriate level for tests and full reporting of outcomes
  - Estimates of effect sizes (e.g. Cohen's  $d$ , Pearson's  $r$ ), indicating how they were calculated

*Our web collection on [statistics for biologists](#) contains articles on many of the points above.*

### Software and code

Policy information about [availability of computer code](#)

- |                 |   |
|-----------------|---|
| Data collection | SoftMax Pro 7.0.2 (Molecular Devices, LLC) was used to measure luminescence in the pseudovirus neutralization assays.   |
| Data analysis   | GraphPad Prism (version 9.2) was used for data visualization and for statistical tests. Cutadapt (version 2.1) was used for processing of raw reads from next-generation sequencing. Bowtie2 (version 2.3.4) was used for alignment of reads to sequences. PISA was used for identifying antibody-spike interface residues. Antibody footprints were optimized by ImageMagick 7.0.10-31. PyMOL (version 2.3.2) was used for RBD mutagenesis analysis and for visualization. |

For manuscripts utilizing custom algorithms or software that are central to the research but not yet described in published literature, software must be made available to editors and reviewers. We strongly encourage code deposition in a community repository (e.g. GitHub). See the Nature Portfolio [guidelines for submitting code & software](#) for further information.

### Data

Policy information about [availability of data](#)

All manuscripts must include a [data availability statement](#). This statement should provide the following information, where applicable:

- Accession codes, unique identifiers, or web links for publicly available datasets
- A description of any restrictions on data availability
- For clinical datasets or third party data, please ensure that the statement adheres to our [policy](#)

Materials used in this study will be made available under an appropriate Materials Transfer Agreement. All the data are provided in the paper. The structures used for analysis in this study are available from PDB under IDs 6ZGE, 7L5B, 6XDG, 7L2E, 7RW2, 7C01, 7KMG, 7CDI, 7KS9, 7LD1, 7RAL, 7LSS, and 6WPT.

## Field-specific reporting

Please select the one below that is the best fit for your research. If you are not sure, read the appropriate sections before making your selection.

Life sciences  Behavioural & social sciences  Ecological, evolutionary & environmental sciences

For a reference copy of the document with all sections, see [nature.com/documents/nr-reporting-summary-flat.pdf](https://www.nature.com/documents/nr-reporting-summary-flat.pdf)

## Life sciences study design

All studies must disclose on these points even when the disclosure is negative.

Sample size	We used similar sample sizes as in previous work (e.g. Wang et al 2021, Nature), which we had previously determined to be sufficient sample sizes for comparisons between groups for these experiments.
Data exclusions	No data were excluded.
Replication	The key results, the resistance of R346K, S371L, B.1.1.529, and B.1.1.529+R346K to monoclonal antibodies in pseudoviruses, and serum neutralization of authentic viruses, were repeated twice independently in technical triplicate with similar results. The results that are shown are representative. Other experiments were conducted in technical triplicate and not repeated.
Randomization	As this is an observational study, randomization is not relevant.
Blinding	As this is an observational study, investigators were not blinded.

## Reporting for specific materials, systems and methods

We require information from authors about some types of materials, experimental systems and methods used in many studies. Here, indicate whether each material, system or method listed is relevant to your study. If you are not sure if a list item applies to your research, read the appropriate section before selecting a response.

### Materials & experimental systems

n/a	Involved in the study
<input type="checkbox"/>	<input checked="" type="checkbox"/> Antibodies
<input type="checkbox"/>	<input checked="" type="checkbox"/> Eukaryotic cell lines
<input checked="" type="checkbox"/>	<input type="checkbox"/> Palaeontology and archaeology
<input checked="" type="checkbox"/>	<input type="checkbox"/> Animals and other organisms
<input type="checkbox"/>	<input checked="" type="checkbox"/> Human research participants
<input checked="" type="checkbox"/>	<input type="checkbox"/> Clinical data
<input checked="" type="checkbox"/>	<input type="checkbox"/> Dual use research of concern

### Methods

n/a	Involved in the study
<input checked="" type="checkbox"/>	<input type="checkbox"/> ChIP-seq
<input checked="" type="checkbox"/>	<input type="checkbox"/> Flow cytometry
<input checked="" type="checkbox"/>	<input type="checkbox"/> MRI-based neuroimaging

## Antibodies

Antibodies used	All of the antibodies used in this study were produced in our laboratory or received from other laboratories. 1-20, 2-15, S309, 2-7, ADG-2, DH1047, 10-40, S2X259, 4-18, and 5-7 were expressed and purified in-house as described previously in Liu et al 2020, Nature. REGN10987, REGN10933, COV2-2196, and COV2-2130 were provided by Regeneron Pharmaceuticals, Brie-196 and Brie-198 were provided by Brie Biosciences, CB6 was provided by Baoshan Zhang and Peter Kwong (NIH), and 910-30 was provided by Brandon DeKosky (MIT).
Validation	All of the antibodies have been validated in previous studies both by binding to SARS-CoV-2 spike and neutralization of SARS-CoV-2 (both pseudovirus and authentic virus), and when applicable, have been confirmed to give similar results as that described in publications by other groups. Specifically, 1-20 and 4-18 were tested in Liu et al 2020, Nature, CB6, Brie-196, 910-30, REGN10933, COV2-2196, LY-CoV555, 2-15, REGN10987, COV2-2130, S309, 2-7, Brie-198, and 5-7 were tested in Wang et al 2021, Nature, and ADG-2, DH1047, 10-40, and S2X259 were tested in Liu et al 2021, bioRxiv.

## Eukaryotic cell lines

Policy information about [cell lines](#)

Cell line source(s)	Expi293 cells were obtained from Thermo Fisher (Catalog #A14527), Vero E6 cells were obtained from ATCC (Catalog# CRL-1586), HEK293T cells were obtained from ATCC (Catalog# CRL-3216), and Vero-E6-TMPRSS2 cells were obtained from JCRB (Catalog# JCRB1819).
Authentication	Cell lines were purchased from authenticated vendors, and morphology was also confirmed visually prior to use.

Mycoplasma contamination

Cell lines tested mycoplasma negative.

Commonly misidentified lines  
(See [ICLAC](#) register)

No commonly misidentified cell lines were used in this study.

## Human research participants

Policy information about [studies involving human research participants](#)

Population characteristics

Population characteristics are described in detail for each individual in Extended Data Table 1 and 2. Convalescent samples had the following ranges: 9-120 days post-symptoms, 45-79 years old, 4/10 female, 6/10 male. We presume all of these individuals were infected with the wild-type strain of SARS-CoV-2 as these samples were collected in Spring of 2020. Vaccinee samples had the following ranges: 6-213 days post-vaccination, 26-78 years old, 12/54 two mRNA-1273 vaccinations, 13/54 two BNT162b2 vaccinations, 9/54 Ad26.COVS2 vaccination, 5/54 two ChAdOx1 nCoV-19 vaccinations, 2/54 three mRNA-1273 vaccinations, 13/54 three BNT162b2 vaccinations, 4/54 previously infected, 8/54 unknown previous infection status, 42/54 uninfected, 31/54 female, 23/54 male.

Recruitment

For convalescent sera, convalescing patients volunteered and were enrolled in an observational cohort study at Columbia University Irving Medical Center in Spring of 2020. For the BNT162b2 and mRNA-1273 vaccinee sera, individuals volunteered and were enrolled in an observational cohort study at Columbia University Irving Medical Center to study the immunological responses to SARS-CoV-2 in individuals who had received COVID-19 vaccines. Ad26.COVS2 and ChAdOx1 nCoV-19 vaccinee serum samples were received from BEI Resources. Self-selection biases may have affected the demographics of the enrolled population, but are not expected to have impacted the results of this study. High titer samples were specifically chosen within each of the serum groups so that fold-change in titer could be better determined, as also discussed in the manuscript.

Ethics oversight

All collections were conducted under protocols reviewed and approved by the Institutional Review Board of Columbia University. All participants provided written informed consent.

Note that full information on the approval of the study protocol must also be provided in the manuscript.